[3] M. McColl, R. J. Pedersen, M. F. Bottjer, M. F. Millea, A. H. Silver, and F. L. Vernon, Jr., "The super-Schottky diode microwave mixer," *Appl. Phys. Lett.*, vol. 28, pp. 159–162, Feb. 1, 1976.
[4] I. Giaever and K. Megerle, "Study of superconductors by electron tunneling," *Phys. Rev.*, vol. 122, pp. 1101–1111, May 15, 1961.
[5] F. A. Padovani and G. G. Sumner, "Experimental study of gold-gallium arsenide Schottky barriers," *J. Appl. Phys.*, vol. 36, pp. 3744–3747, Dec. 1965.
[6] M. F. Millea, M. McColl, and C. A. Mead, "Schottky barriers on GaAs," *Phys. Rev.*, vol. 177, pp. 1164–1172, Jan. 15, 1969.
[7] F. A. Padovani, "Graphical determination of the barrier height and excess temperature of a Schottky barrier," *J. Appl. Phys.*, vol. 37, pp. 921–922, Feb. 1966.
[8] T. J. Viola, Jr., and R. J. Mattauch, "High-frequency noise in Schottky-barrier diodes," *Proc. IEEE*, vol. 61, p. 393, Mar. 1973.
[9] S. Weinreb and A. R. Kerr, "Cryogenic cooling of mixers for millimeter and centimeter wavelengths," *IEEE J. Solid-State Circuits (Special Issue on Microwave Integrated Circuits)*, vol. SC-8, pp. 58–63, Feb. 1973.
[10] A. R. Kerr, "Low-noise temperature and cryogenic mixers for 80–120 GHz," *IEEE Trans. Microwave Theory Tech.*, vol. MTT-23, pp. 781–787, Oct. 1975.
[11] G. C. Messenger and C. T. McCoy, "Theory and operation of crystal diodes as mixers," *Proc. IRE*, vol. 45, pp. 1269–1283, Sept. 1957.
[12] H. C. Torrey and C. A. Whitmer, *Crystal Rectifiers*, MIT Radiation Lab. Series, vol. 15. New York: McGraw-Hill, 1948.
[13] A. A. M. Saleh, "Theory of resistive mixers," Ph.D. dissertation, MIT, Cambridge, MA, 1970.
[14] J. Bardeen, L. N. Cooper, and J. R. Schrieffer, "Theory of superconductivity," *Phys. Rev.*, vol. 108, pp. 1175–1204, Dec. 1, 1957.
[15] S. Berman, "The BCS differential conductance for a metal-insulator-superconductor tunneling junction," *Tech. Rept. 1, NSF-GP1100*, University of Illinois, Urbana, 1964.
[16] M. McColl, M. F. Millea, and C. A. Mead, "Zero-bias contact resistances of Au-GaAs Schottky barriers," *Solid-State Electron.*, vol. 14, pp. 677–683, 1971.
[17] M. McColl and M. F. Millea, "Schottky barriers on InSb," *J. Electronic Mat.*, vol. 5, pp. 191–207, Apr. 1976.
[18] H. M. Day, A. C. MacPherson, and E. E. Bradshaw, "Multiple contact Schottky barrier microwave diode," *Proc. IEEE*, vol. 54, pp. 1955–1956, Dec. 1966.
[19] A. R. Kerr, "Anomalous noise in Schottky diode mixers at millimeter wavelengths," *IEEE S-MTT Symposium Digest*, International Microwave Symposium, Palo Alto, CA, pp. 318–320, 1975.
[20] C. A. Mead and W. G. Spitzer, "Fermi level position at semiconductor surfaces," *Phys. Rev. Lett.*, vol. 10, pp. 471–472, June 1, 1963.
[21] M. F. Millea, M. McColl, and A. H. Silver, "Electrical characterization of metal/InAs contacts," *J. of Electronic Mat.*, vol. 5, pp. 321–340, June 1976.
[22] H. Miki, K. Segawa, M. Otsubo, K. Shirahata, and K. Fujibayashi, "Growth of $In_{1-x}Ga_xSb$ by liquid phase epitaxy," *Proc. 5th Int. Symp. Gallium Arsenide and Related Compounds, 1974*, London and Bristol: Institute of Physics, 1975, pp. 16–21.
[23] K. Kajiyama, Y. Miyushima, and S. Sakata, "Schottky barrier height of n-$In_xGa_{1-x}As$ diodes," *Appl. Phys. Lett.*, vol. 23, pp. 458–459, Oct. 15, 1973.

The Measurement of Noise in Microwave Transmitters

J. ROBERT ASHLEY, SENIOR MEMBER, IEEE, THOMAS A. BARLEY, MEMBER, IEEE, AND GUSTAF J. RAST, JR.

Invited Paper

***Abstract*—A tutorial review of the basis for transmitter noise measurements shows that noise is best described and measured as AM and FM noise. The determination of RF spectrum is done by calculation after the AM and FM noise are known. The contribution of AM noise to RF spectrum shape is determined by the power spectral density shape of the AM noise. The contribution of FM noise to RF spectrum is to make the shape that of an *RLC* circuit resonant response rather than a δ function with a sideband structure. The measurement of AM noise is done with a direct detector diode. The measurement of FM noise for frequencies above 5 GHz is done with a discriminator based on a one-port cavity resonator. The measurement of FM noise below 5 GHz is done with an improved transmission line discriminator which is described in detail. Measurement of low-power low-noise signal sources is made possible with an injection-locked oscillator for a preamplifier to the discriminator. The most widely used baseband analyzer is the constant bandwidth superheterodyne wave or spectrum analyzer. Most differences in measurement results are resolved by understanding the baseband analyzers. At least the baseband spectrum analysis of transmitter noise measurements can be automated with worthwhile savings in time and improvement of documentation.**

Manuscript received September 1, 1976; revised September 20, 1976.
J. R. Ashley is with the Department of Electrical Engineering, University of Colorado, Colorado Springs, CO 80907.
T. A. Barley and G. J. Rast, Jr., are with DRDMI-TER, U.S. Army Missile Research and Development Command, Redstone Arsenal, AL 35809.

I. Background Concepts

NOISE in a microwave transmitter is an unwanted kind of signal which degrades the ability of the system to transmit communications or other information. We must include both stochastic signals and coherent spurious signals—usually related to bias supply ripple or mechanical vibration—in our thinking about transmitter noise. In the first stages of receiving systems, we are usually concerned with a ratio of desired signal to noise in the order of unity. In a transmitter, the ratio of carrier to noise is on the order of 10^3 or more. Most of the amplifying or oscillating devices in a transmitter are operating in a saturated mode; thus some of the linear system theory ideas that are so useful in the study of receiving systems must be used with care in studying a transmitter system.

The user of a microwave transmitter also will be using a detection system which may respond to either amplitude modulation or angle modulation (an FM discriminator), but not often both. His essential question is, "How much of the noise in a transmitter will come out of my detection system?" The kind of a detector being used will determine if the user is concerned with what has come to be called "FM noise"

or "AM noise." Fortunately, the study of oscillator theory as pioneered by Middleton [1], Mullen [2], and others yields answers in terms of FM noise or AM noise; and even more fortunately, the measurement techniques which yield the best data are based on separately detecting AM noise and FM noise [3], [4].

The measurement of transmitter noise is accomplished by applying a suitable sample of the output to detectors which respond to either AM or FM. It is easy to visualize an AM detector which rejects a moderate amount of incidental FM on the signal being tested. It is not so easy to visualize a microwave discriminator without a limiter stage rejecting incidental AM on the signal being tested; yet, the cavity resonator discriminators of Marsh and Clare [5], Ashley *et al.* [3], and the new transmission line discriminators of Ashley *et al.* [6], do indeed reject incidental AM. Any competitive methods must reject the unwanted form of modulation in measuring the desired form.

Current microwave transmitters include those with a simple high-power oscillator (such as a magnetron) as the only device, those which include direct microwave oscillators (reflex klystrons, TEO, IMPATT), driving amplifiers (amplitron, klystron, TWT, locked IMPATT oscillator, transistor), and those which synthesize the microwave signal from sources controlled by VHF or UHF crystal oscillators and then increase the power with amplifiers. To measure noise in transmitters, we must be able to study direct oscillators, amplifiers, and the VHF and UHF oscillators, amplifiers, and frequency multipliers.

The range where the demodulated noise must be studied varies with the applications. Doppler radar systems are degraded by excessive noise in the modulation range 10 Hz–100 kHz, and the usual noise specification covers a significant portion of this range. Communications systems using FM multiplex the subcarriers into a band typically 10 MHz wide, and this sets the upper limit on the measurement of demodulated noise. These modulation frequencies are sometimes described as distance from the carrier with an implied idea of the RF spectrum spread.

In FM communications, the nonlinearity in amplifiers can cause cross modulation of multiplexed subcarriers which is a form of distortion. This will appear in the system output as unwanted signals in the individual channels. This meets the definition of noise as being unwanted, but we will not treat the problem further in this work.

Understanding noise and the mathematics for studying noise requires some careful definitions and explanations. Some of the intuitive ideas about noise based on modulation theory using sinusoids only are imprecise to say the least, and we advise you to not avoid the next section which gives some of the concepts needed.

II. Modulation Noise Relationships

Most of the relationships to be given here are tersely abstracted from [7] and [8]. Naturally, we leave the proofs and many details to the References.

For amplitude modulation transmitters, the output can be written

$$v(t) = A_0[1 + \lambda V_s(t)] \cos(\omega_c t + \phi) \tag{1}$$

where

- t time;
- A_0 unmodulated amplitude (peak volts);
- ω_c $2\pi\nu_c$ = carrier frequency (radians per second);
- ν_c carrier frequency (hertz);
- ϕ phase constant usually set to zero by proper choice of coordinates;

and $\lambda V_s(t) \leq 1$ is the information to be communicated. We are interested in the noise floor which exists when $V_s(t) = 0$. Thus we replace $\lambda V_s(t)$ by $N_A(t)$ where $N_A(t)$ is the AM noise and must be treated as a random variable.

To distinguish the frequency variable near the carrier from frequency in the baseband region where modulation noise must be described, we shall use the lower case Greek nu (ν) for frequency (hertz) near the carrier frequency ν_c. In the baseband region from zero to a few megahertz, we shall use f to designate frequency (hertz).

Similarly, for angle modulated transmitters, the output can be written

$$v(t) = A_0 \cos(\omega_c t + \Phi(t) + \phi) \tag{2}$$

where the information to be transmitted is carried in the instantaneous phase $\Phi(t)$. The instantaneous frequency ν_i of this signal is

$$\nu_i = \frac{d}{dt}(\omega_c t + \Phi(t) + \phi) = \omega_c + \dot{\Phi}(t). \tag{3}$$

We are interested in the residual $\Phi(t)$ or $\dot{\Phi}(t)$ for the unmodulated state which we will call $\Phi_N(t)$ or $\dot{\Phi}_N(t)$. Again, $\Phi_N(t)$ must be considered as a random variable. From a measurement standpoint, it is fortuitous that we usually measure $\dot{\Phi}_N(t)$ with a discriminator and can integrate the result to find $\Phi_N(t)$.

Combining these equations, the signal from an unmodulated transmitter can be written

$$v(t) = A_0(1 + N_A(t)) \cos(\omega_0 t + \Phi_N(t) + \phi) \tag{4}$$

where

$$|N_A(t)| \ll 1 \tag{5}$$

and

$$|\Phi_N(t)| \ll 1. \tag{6}$$

Our task is to learn something about $N_A(t)$ and $\Phi_N(t)$ by measurements made on $v(t)$.

Except for components caused by bias supply ripple or deterministic mechanical vibrations, the signals $N_A(t)$ and $\dot{\Phi}_N(t)$ are not deterministic and must be studied from a statistical point of view. Any dc average is absorbed in either A_0 or ω_c; so, it is appropriate to consider that $N_A(t)$ and $\Phi_N(t)$ have zero mean and study the density function, variance, autocorrelation function, and band-limited spectrum.

The probability density function for $N_A(t)$ or $\Phi_N(t)$ is difficult to measure to say the least. It is usually assumed by implication to be Gaussian for the simple reason that this is the mathematically best known function. In terms of physical processes in oscillators and amplifiers, this is not an unreasonable assumption.

The usual definition of an autocorrelation function can be applied to $A_N(t)$ and $\Phi_N(t)$.

$$R_A(\tau) = \lim_{T\to\infty} \frac{1}{2T} \int_{-T}^{T} N_A(t)N_A(t+\tau)\,dt \tag{7}$$

$$R_\phi(\tau) = \lim_{T\to\infty} \frac{1}{2T} \int_{-T}^{T} \Phi_N(t)\Phi_N(t+\tau)\,dt \tag{8}$$

$$\tau = t_2 - t_1 \tag{9}$$

and for the real random variables $N_A(t)$ and $\Phi_N(t)$

$$R(-\tau) = R(\tau). \tag{10}$$

The autocorrelation function is used as the mathematical link between the time domain and frequency domain descriptions of random variables. The Wiener–Khintchine theorem states that for ergodic and well-behaved real processes the power spectral density $S(f)$ and the autocorrelation functions $R(\tau)$ are a Fourier transform pair

$$S(f) = \int_{-\infty}^{\infty} R(\tau)\cos(2\pi f\tau)\,d\tau \tag{11}$$

$$R(\tau) = \int_{-\infty}^{\infty} S(f)\cos(2\pi f\tau)\,df. \tag{12}$$

The power spectral density is an even, real function and nonnegative

$$S(-f) = S(f) \tag{13}$$

$$S(f) \geq 0. \tag{14}$$

The power spectral density of the noise modulations is band limited to a small fraction of the carrier frequency by resonant circuits in the signal generation source.[1] This limited band is usually termed the "baseband."

In terms of the measurement problem, applying the source to demodulators as shown in Fig. 1 yields voltages proportional to $N_A(t)$, $\Phi_N(t)$, and $\dot{\Phi}_N(t)$ which are functions of time. The simplest data processing in the time domain is to use a cathode ray or mechanical oscillograph to record instantaneous amplitude, phase, or frequency versus time. The records are often called "stability" although the word instability might be more appropriate. In terms of frequency or phase instability, the time domain processing can be quite sophisticated if long-term stability (time period of days or more) is important—as in timekeeping applications. The use of computing counters to determine the sigma versus tau characteristic is well described by Shoaf *et al.* [15].

In theory, it should be possible to apply the output of the demodulators to autocorrelation computing equipment.

[1] This is not true for traveling-wave tube amplifiers or backward wave tube oscillators.

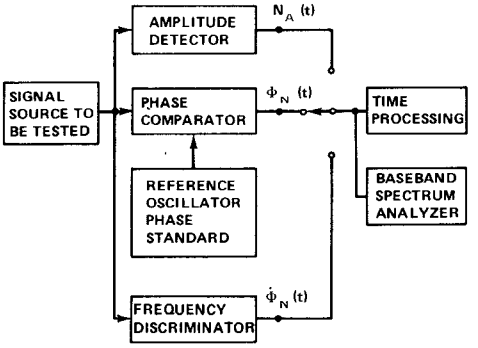

Fig. 1. Schematic representation of modulation noise measurements.

We do not know of published results of such an experiment. One experiment which would be of great significance in oscillator noise theory would be to determine the cross correlation between amplitude and phase noise modulation.

Since most microwave transmitters are used in either radar or communication systems, the most useful analysis of the modulation noise is in the frequency domain. The baseband analysis equipment is usually called a spectrum analyzer if frequency is automatically swept through and a wave analyzer if the frequency is manually set. These equipments are of sufficient importance that we devote a later section to their discussion.

You may wonder why nothing has been said to this point about the microwave spectrum of $v(t)$. The main reason is that the measurement of the signal spectrum will not predict the effects of transmitter noise on the amplitude or angle demodulators in the receiver—from the signal spectrum alone it is not possible to determine if a particular sideband is caused by N_A or $\Phi_N(t)$. If one needs to know the spectrum structure in the region of the carrier, he will usually find it well hidden under the noise floor of the spectrum analyzer. Thus $N_A(t)$ and $\Phi_N(t)$ must be measured and used to compute the near carrier spectrum.

This is not to deny the usefulness of a microwave spectrum analyzer in studying transmitter noise. Observation of spurious signals at subharmonic, harmonic, and unwanted mixing product frequencies is best done with these powerful tools. We will also make much use of the microwave spectrum analyzer in the alignment and calibration of AM and FM noise measuring equipment.

The theory required to understand the near carrier spectrum structure requires the most difficult mathematics of this paper but should not be avoided.

III. The Spectrum of Modulated Signals

Our approach to this topic paraphrases that given by Middleton [7] by considering low index AM, ϕM, and FM separately and then combining results for simultaneous AM and FM. Throughout, the use of autocorrelation functions and the Wiener–Khintchine theorem makes the results apply to both deterministic (usually sinusoidal) and stochastic modulation signals. First, for amplitude modulation only,

$$v(t) = A_0(1 + \lambda V_M(t))\cos(2\pi\nu_c t) \tag{15}$$

where $N_A(t) = \lambda V_M(t)$. With just a little bit of work, the spectrum $S_{RF}(v)$ is found from ([7], eq. 12.10b)

$$S_{RF}(v) = A_0{}^2\delta(v - v_c) + \lambda^2 A_0{}^2 \int_0^\infty R_M(\tau) \cos 2\pi(v - v_c)\tau \, d\tau \tag{16}$$

where $R_M(\tau)$ is the autocorrelation function of the modulation $V_M(t)$. The δ-function $\delta(v - v_c)$ indicates a spectral line at v_c. If $V_M(t) = \cos 2\pi f_a t$ and $\lambda < 1$, then

$$S_{RF}(v) = \frac{A_0{}^2}{2}\delta(v - v_c) + \frac{A_0{}^2\lambda^2}{8}\delta(v - (v_c + f_a)) + \frac{A_0{}^2\lambda^2}{8}\delta(v - (v_c - f_a)) \tag{17}$$

which is the familiar carrier with a pair of side frequencies located at $v_c \pm f_a$. If V_M is a more complex signal which can be expressed as a Fourier series of sinusoids, then pairs of side frequencies will appear for each Fourier component. There will be no cross products as long as the total modulation index is kept less than 1 (i.e., no overmodulation).

A most useful result can be deduced for the case of any form of low index amplitude modulation. If we were to find the spectrum of V_M from its autocorrelation function, we would evaluate

$$S_{AM}(f) = 2\int_0^\infty R_M(\tau) \cos 2\pi f\tau \, d\tau \tag{18}$$

while the sideband portion $S_{SB}(v)$ of (16) requires evaluation of

$$S_{SB}(v) = \int_0^\infty R_M(\tau) \cos 2\pi(v - v_c)\tau \, d\tau. \tag{19}$$

An obvious change of variable yields

$$S_{RF}(v) = \frac{A_0{}^2}{2}\delta(v - v_c) + \frac{\lambda^2 A_0{}^2}{4} S_{AM}(v - v_c) \tag{20}$$

which tells us that the spectrum of the modulating signal is shifted from being symmetrical about $f = 0$ to being symmetrical about $v = v_c$. Therefore, if we can measure the spectrum of the AM noise $S_{AM}(f)$, we can make a prediction of the contribution of AM noise to the RF spectrum using (20).

This important concept is illustrated by Fig. 2. The measured noise spectrum of the AM, $S_{MAM}(f)$, is shown as it would be measured in Fig. 2(a). This is a power spectral density for the baseband range. Mathematically, we must carry the negative frequency portion of the spectrum which is the mirror image of the positive portion as shown in Fig. 2(b). The fact that $S_{AM}(f)$ is the AM spectrum means that the RF spectrum can be found by translating $S_{AM}(f)$ to the regions near $\pm v_c$ and adding the δ-function representing the carrier. This is illustrated in Fig. 2(c). Our example AM noise spectrum has both δ-functions to represent sinusoids and a continuous portion to represent random noise.

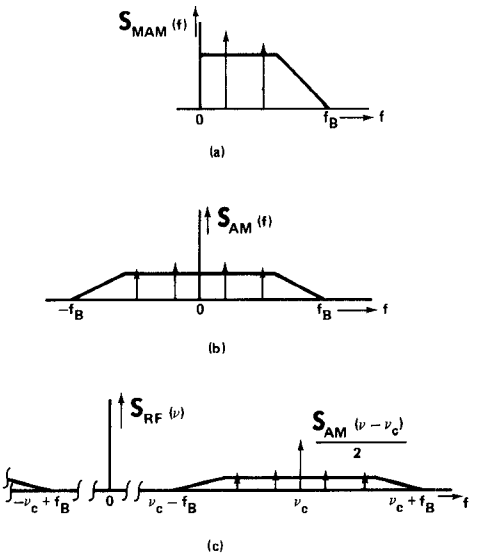

Fig. 2. (a) Measured spectrum of AM noise. (b) Mathematical representation of AM noise. (c) RF spectrum caused by AM noise.

For the case of angle modulation only, the RF signal can be written

$$v(t) = A_0 \cos(2\pi v_c t - \Phi(t)) \tag{21}$$

where $\Phi(t)$ is chosen for phase or frequency modulation as

$$\Phi(t)_{\phi M} = D_\phi V_M(t) \tag{22}$$

$$\Phi(t)_{FM} = D_F \int^t V_M(t') \, dt'. \tag{23}$$

Here D_ϕ has units of radian/volt and D_F has units of angular frequency (radian/second) per volt. For the case where V_M is sinusoidal, let

$$\Phi(t) = \mu_{\phi M} \cos 2\pi f_a t \tag{24}$$

for phase modulation and

$$\Phi(t) = \mu_{FM} \sin 2\pi f_a t \tag{25}$$

where $\mu_{\phi M} = \Delta\phi$, the magnitude of the phase deviation and $\mu_{FM} = \Delta v/f_a$, the frequency deviation divided by the modulation frequency are the appropriate modulation indices for ΦM and FM. With more than a little bit of work and Bessel function manipulation, Middleton ([7], eq. 14.10b f.f.) finds the autocorrelation function and the spectrum

$$R_V(\tau) = \frac{A_0{}^2}{2} J_0\left(2\mu \cos\frac{2\pi f_a \tau}{2}\right) \cos 2\pi v_c \tau \tag{26}$$

$$S_{RF}(v) = \frac{A_0{}^2}{2} \cdot \sum_{m=0}^{\infty} J_m{}^2(u)\{\delta(v - (v_c + mfa)) + \delta(v - (v_c - mfa))\} \tag{27}$$

where J_m is an mth order Bessel function. This is the familiar result with the multitude of side frequencies for large μ. If $\mu < 0.01$, only the $m = 1$ side frequencies are significant and the approximation $J_1(x) = x/2$ is useful. This theory

is the basis for calibration of the discriminators used for FM noise measurements.

If more than one sinusoid is present in the modulation signal, then additional side frequencies are added for low values of μ. For large μ, the nonlinearity of angle modulation causes some cross coupling of the modulation. For example, if two sinusoids at 300 and 1000 Hz angle modulate a carrier, the spectrum will have components located at ± 1300, 1600, 2300, 2900 Hz, etc., away from the center frequency as well as at the harmonies of 300 and 1000 Hz. These facts and the expression $\mu_{FM} = \Delta v/f_a$ should make us expect trouble when the modulation is not deterministic.

The theory does not disappoint our expectation. The limiting behavior for small modulation is fortunately all we need to consider in this study. Since we are concerned with the case where the modulation is just the residual noise in the source, we can take Middleton's equations [7, sec. 14.2-1] and abandon higher order terms with great vigor because Φ is quite small. For phase modulation,

$$R_V(\tau) \approx \frac{A_0^2}{2} \cos 2\pi v_c \tau \{1 + R_{\phi M}(\tau)\} \tag{28}$$

which is Fourier transformed to find the RF spectrum

$$S_{RF}(v) \approx \frac{A_0^2}{2} \delta(v - v_c) + \frac{A_0^2}{2} \int_0^\infty R_{\phi M}(\tau) \cos 2\pi v_c \tau \cos 2\pi v \tau \, d\tau. \tag{29}$$

In the integral, the identity for $\cos A \cos B$ can be used, a term in $\cos 2\pi(v_c + v)$ abandoned by a stationary phase argument, and the same clever substitution used in the AM theory invoked to show

$$S_{RF}(v) = \frac{A_0^2}{2} \delta(v - v_c) + \frac{A_0^2}{4} S_{\phi M}(v - v_c). \tag{30}$$

We should be overjoyed with this result because it shows the same sort of limiting behavior as we found in the AM case. A carrier line is the center frequency for the symmetrical phase modulation spectrum which is unchanged in spectral shape. Thus we might measure $S_{\phi M}(f)$ and very quickly translate it to the RF spectrum.

Our joy begins to fade when we look at typical measurements of $S_{\phi M}(f)$ and study oscillator theory. Leeson [17] shows general forms for $S_{\phi M}(f)$ which show a behavior below about 1 kHz which is of the order $1/f^2$ or $1/f^3$. Going back to the theory with this knowledge of $S_{\phi M}(f)$ shows that all our approximations were not very well justified. Those who use the "theorem" implied in (30) would be in for a rude shock if they could *measure* $S_{RF}(v)$ for a signal where $S_{\phi M}(f)$ is known.

The true understanding of the RF spectrum for small angle modulation comes from the study of limiting forms for FM noise modulation. The classic reference is Mullen and Middleton [18] although the work is well documented in Middleton's book [7, sec. 14.2-1]. The root of the mathematical trouble is in the value of an integral

$$L = \int_0^\infty \frac{S_{FM}(f)}{4\pi^2 f^2} \, df \tag{31}$$

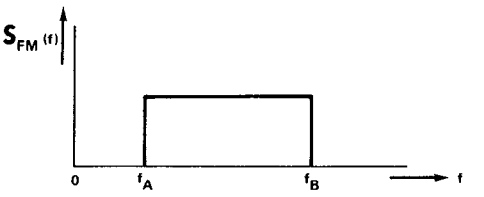

Fig. 3. An idealized FM noise spectrum.

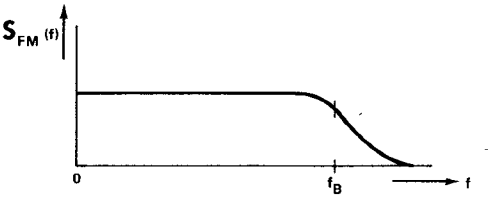

Fig. 4. A more typical FM noise spectrum.

needed in finding the autocorrelation function. There are two cases which have been worked through. The first case is for an idealized spectrum for $S_{FM}(f)$ sketched in Fig. 3. When the noise spectrum does not extend to zero frequency, $L < \infty$ and the limiting form for the RF spectrum is [7, eq. 14.42b]

$$S_{RF}(v) = \frac{A_0}{2} \left[\delta(v - v_c) + \frac{1}{2} \frac{S_{FM}(v - v_c)}{(v - v_c)^2}\right] \tag{32}$$

which is valid only for

$$|v - v_c| < f_b. \tag{33}$$

This is the kind of a result we would intuitively expect from using sinusoidal modulation theory for the small deviation case. Since this idealized spectrum S_{FM} does not go to zero frequency, the analogous sinusoidal modulation index $\Delta v/f_A$ does not go to infinity and cause our intuition trouble.

The real world case corresponds to the FM noise spectrum sketched in Fig. 4. Even this sketch is idealized because the oscillator should show a $1/f$ spectral shape near $f = 0$. Still, if the FM noise spectrum is constant as $f \to 0$, then the integral L of (31) diverges. By a different mathematical route Middleton [7, eq. 14.45] obtains the RF spectrum as

$$S_{RF}(v) = \frac{\gamma A_0^2}{\gamma^2 + 4\pi^2(v - v_c)^2} + \text{correction term.} \tag{34}$$

The correction term is significant only in the "tails" of the spectrum, where

$$|v - v_c| > f_b. \tag{35}$$

There is a surprising physical significance in this development. In the region

$$|v - v_c| < f_b \tag{36}$$

the shape of $S_{FM}(v)$ does not appear in the leading term for the spectrum. Also, there is not a δ-function in (34) so we cannot talk of a carrier for computing carrier-to-noise sideband ratios. Instead of the discrete carrier and sideband structure of AM or overly idealized angle modulation, the real world signal sources have a spectral shape resembling the resonant response of a series L–R–C circuit shown in Fig. 5. The width of this spectral "line," is γ/π where γ is a

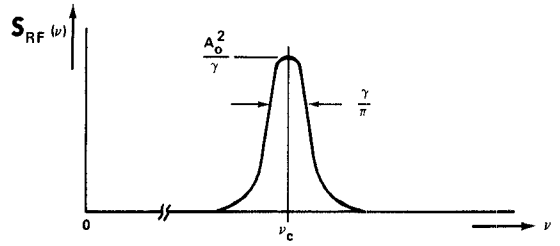

Fig. 5. The limiting form for the spectrum with low FM noise of the shape given in Fig. 4.

measure of the total power in the FM noise spectrum, that is, a factor proportional to the area under the $S_{FM}(f)$ curve. In practice, the linewidth is of the order of a few hertz at the most and cannot be resolved with commercially available RF spectrum analyzers which might have a minimum bandwidth of 10 Hz. (Also, the noise floor in the spectrum analyzer is too high to see anything important.) This is why the failure of (34) to match the intuitive extrapolation of sinusoidal FM theory has not been detected by measurement.

The theory just presented is not the conventional wisdom widely practiced for computing spectrum.[2] One cannot help but wonder why someone has not discovered the error through measurement. With 20-20 hindsight, we can see one area where the correct spectrum computation explains a good result. As documented by Risley *et al.* [13] and McDonald *et al.* [26], a research program to beat the output of *X*-band signal sources with various laser radiations in a Josephson junction has been carried out at the National Bureau of Standards, Boulder, CO. The first experiment used a reflex klystron electronic phase locked to a UHF crystal oscillator. Only a beat with the 0.964-THz line from an HCN laser had been detected. Substitution of a transmission cavity stabilized klystron made possible detection of a beat of the 401-st harmonic of the klystron frequency with a 3.82-THz water-vapor laser. Misuse of (32) would predict similar spectrums for the two different klystron systems within the 8-kHz bandwidth of the receiving system used. Correct computation of the RF spectrum explains why the lower FM noise above 10 kHz in the cavity stabilized klystron made possible the detection of the higher harmonic.

The case when FM and AM are present simultaneously deserves only brief comment. For the sinusoidal case, the result of simultaneous amplitude and angle modulation is to destroy the symmetry of the RF spectrum. For our concern with transmitter noise measurements, this asymmetrical spectrum when seen while looking at calibration side frequencies means that the pure amplitude or angle modulation needed for calibration is not present and the calibration equipment must be realigned.

The unmodulated RF output of a microwave transmitter or of any RF signal source is going to have both AM and FM noise simultaneously present. This will give basically three terms to compute to find the RF spectrum: 1) a component caused by the FM noise, 2) a component caused by the AM noise, and 3) a component caused by the cross correlation of the AM and the FM noise. For frequencies within a few kilohertz of the carrier region, the FM noise term dominates. For frequencies more than a few tens of kilohertz from the carrier region, the AM term dominates. The cross-correlation term would be found by applying the Wiener–Khintchine theorem to the cross-correlation function. Middleton [7, sec. 14.3-1] shows that the computed effect is to skew the spectrum. Thus the result is of diagnostic value for transmitters (such as counter-measures jammers) which use large index noise modulation to produce wideband noise as the primary output. If the spectrum is asymmetrical, then the modulation is not pure amplitude or angle. For the low residual level of the AM and FM noise in an unmodulated transmitter, a measurement of the cross-correlation function would be required before anything definitive could be said about the importance of this term in the RF spectrum computation.

What conclusions can we reach from this diversion into communications theory? In relation to our topic of transmitter noise measurements, these conclusions must include the following.

1) Both the nature of noise in transmitters and the measurement equipment available dictate the measurement of AM noise, and ϕM or FM noise.

2) The theory of amplitude or angle modulation by sinusoids gives the basis for alignment and calibration of noise measurement equipment.

3) A microwave spectrum analyzer is useful for detecting spurious outputs several megahertz from the carrier region in a transmitter but cannot yield sufficient information about the noise modulation of the output.

4) A microwave spectrum analyzer is needed for alignment and calibration of AM and angle modulation noise measurement equipment.

5) Estimation of the contribution of AM noise to the RF spectrum is straightforward [see (20)] and has no booby traps.

6) Estimation of the contribution of angle modulation noise to the RF spectrum is not straightforward [see (34)] and many unknowingly fall into a serious booby trap [using (32)].

7) FM or ϕM noise specifications based on a few numbers such as carrier-to-noise ratio at specified frequency (or frequencies) from the carrier are not sufficiently precise. A curve showing maximum limits of the angle modulation noise must be specified for completeness.

8) If you are asked to find the RF spectrum in the region near the carrier, you should ask why.

9) If there is a good reason for determining the spectrum in the region near the carrier, carefully measure AM noise and ϕM or FM noise and then compute. (You will not find enough detail in this paper to make the computations. See Middleton [7].)

10) One must be careful about extrapolating theory based on sinusoids only to a situation where random noise is involved.

[2] The majority of spectrum computations described in books, journals, and specifications correspond to the unjustified use of (30) and (32).

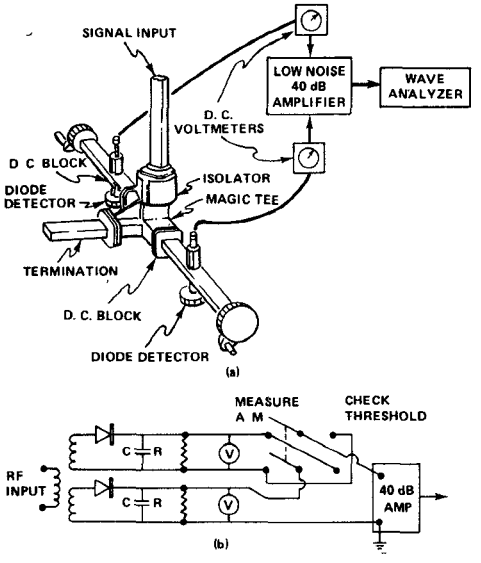

Fig. 6. (a) The balanced AM detector. (b) Its low-frequency equivalent circuit.

With those ten conclusions, we must now get back to our main topic of measuring transmitter noise.

IV. Measurement of AM Noise

The first measurement to consider is determining $N_A(t)$ in (5). In practice, the measurement yields the spectral description $S_{AM}(f)$. There has been no significant advance in this technique since the reports by Ashley *et al.* [3] and Ondria [4] in the September 1968 Special Issue on Noise of this TRANSACTIONS. As reported there, a direct detector diode is simpler than a superheterodyne demodulator and has a lower threshold. For measuring noise and determining the threshold or noise floor of the measurement, a double diode circuit such as the one shown in Fig. 6 is convenient. The two detector mounts are insulated for dc and baseband frequencies up to several megahertz by plastic shims between the mounts and the main portion of the waveguide. This allows the diodes to be connected in series aiding or opposing as indicated in the low-frequency equivalent circuit of Fig. 6(b). The dc blocks account for the two secondary windings on the equivalent circuit. The two capacitors labeled C are actually cable capacity and the resistors R are 1–10 kΩ each. At this impedance level, we have not been troubled with interference at the power line frequency either in or out of shielded rooms.

Silicon point contact diodes can be operated at about 1 V dc without exceeding the peak inverse voltage limit. Since this is a high-level detection application and the noise from the diodes sets the power limit, we can improve the threshold by increasing the power applied to the diodes. Here the higher peak inverse voltage that can be applied to a Schottky-barrier diode makes it a superior device for AM measurements. (Note that detector mounts designed for point contact diodes will not function properly with Schottky-barrier diodes because of the difference in I–V characteristics of the two kinds of diodes. This can be remedied over a limited but adequate microwave bandwidth either with a slide screw tuner or by inserting an adjustable capacitive post in the diode mount at a point $0.3\lambda_g$ in front of the diode.)

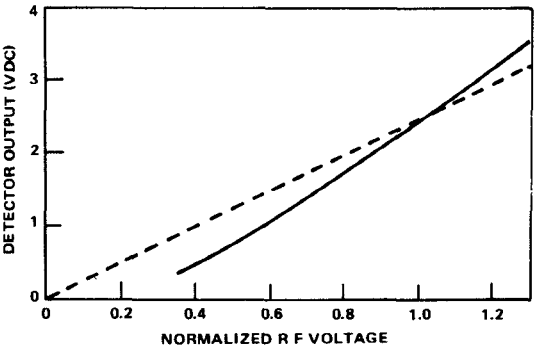

Fig. 7. Schottky-barrier diode detection characteristics (HPA2627 diodes at 10 GHz).

Depending on the type of detector used, a signal level of +1 to 5 dBm is applied to the detector input and the two mounts are tuned for maximum dc voltage output. Both detectors should be adjusted as nearly as possible for identical operation. Then data are taken to determine the detector characteristics of Fig. 7. The abscissa of this curve is obtained by normalizing the RF voltage with respect to the voltage at the operating point. The RF input to the detector is controlled by a precision waveguide attenuator. The ratio of the slope at the operating point to the slope of a line from the origin to the operating point gives a correction factor C which is used in (37). The correction factor for the diode characteristic of Fig. 7 amounts to 3.5 dB at an operating level of 2.45 V.

In stating the correction factor in this simple form, we have made two assumptions about the equipment. First, the microwave bandwidth of the detector mounts is much wider than either the maximum deviation or the highest amplitude modulation frequency to be measured. Second, the ac input impedance of the video amplifier is greater than $20R$.

Once the slope correction has been determined, data are taken from the wave analyzer to determine the AM noise power spectral density:

$$\mathrm{AM}(f) = 20 \log_{10} V_{\mathrm{AM}}(f) - 20 \log_{10} V_{\mathrm{REF}} - 20 \log_{10} C - G_v - 6 - 10 \log_{10} B_N \quad (37)$$

where

- $\mathrm{AM}(f)$ amplitude modulation noise-to-carrier ratio in a 1-Hz bandwidth (decibels);
- $V_{\mathrm{AM}}(f)$ reading of wave analyzer (rms volts);
- V_{REF} dc voltage for each detector in Fig. 6;
- B_N noise bandwidth of the wave analyzer (hertz);
- G_v gain of the video amplifier (decibels);
- C correction factor derived from Fig. 7;
- f modulation frequency, read from wave analyzer (hertz).

The 6-dB factor is used to account for the two detectors operating in series. If a single diode detector is used, this 6-dB factor is omitted.

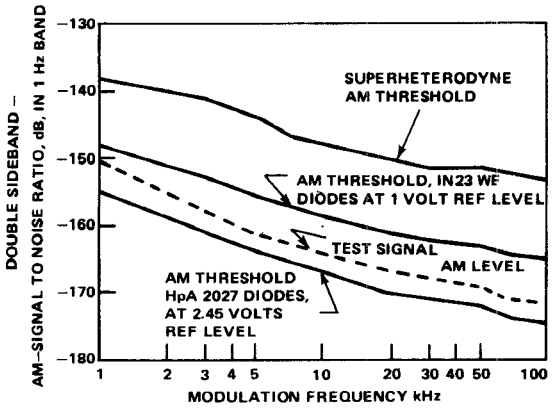

Fig. 8. The AM threshold for a superheterodyne receiver, silicon point contact diodes (IN23WE), and Schottky-barrier diodes (HPA2627).

The quantity AM(f) is the ratio of $S_{AM}(f)$ to carrier power expressed in decibels. This is often described as the double-sideband noise-to-carrier ratio because the use of (20) means that in the RF spectrum, this AM noise will appear one-half on each side of the carrier.

In practice, we have observed that the most frequent failing is neglecting to determine the measurement threshold.[3] Thus, if one attempts an AM noise measurement with a single-ended diode AM demodulator, he should check the typical threshold curves for his demodulator device as given by Fig. 8. If measured data are within 6 dB of expected threshold, then a balanced detector such as the one illustrated for waveguide in Fig. 6 needs to be constructed. The test for threshold shown in Fig. 6(b) consists of operating the individual diodes in series opposition so that the AM on the test signal is mostly canceled. Here, the balance of the diodes is most important and must be tested under RF excitation. One easy method is to apply intentional sinusoidal AM on the test signal and match the detectors to yield minimum output at the AM frequency. The first intuition would be to balance the detectors by tuning adjustment. This tends to cause unbalance for modulation frequencies above 100 kHz, and a better way is to adjust the sizes of the load resistors R to balance the detector system. A plot of noise spectrum from the detector is a good indication of threshold. Reconnecting the diodes to series aiding then gives an output which is the sum of threshold noise and AM noise. If the output is within 2–10 dB of threshold, then a correction

$$V_{AM}(f) = \sqrt{V_{AMM}^2(f) - V_{ATH}^2(f)} \tag{38}$$

where

$V_{AM}(f)$ corrected noise voltage;
$V_{AMM}(f)$ uncorrected AM noise data;
$V_{ATH}(f)$ threshold data;

improves accuracy. Note that the correction must be done on a power spectral density basis before expressing the answer as an AM noise-to-carrier ratio in decibels.

[3] In a conversation at the 1976 IEEE-MTT-S International Symposium, Dr. J. Ondria made a similar observation.

Some of our practical experience with AM noise measurements may help you save time in the laboratory. If you are measuring a source which has a known relatively high AM noise, such as IMPATT amplifiers and oscillators or transmitter TWT amplifiers, then the simple single-ended silicon point contact diode is adequate, available, and reliable. The least expensive versions of 1N21 or 1N23 sorts of diodes are just as useful in this application as those which are sorted for best superheterodyne noise figure.

If you are measuring a source with relatively low AM noise, such as klystron oscillators or transferred electron oscillators (TEO's) using GaAs diodes (Gunn diodes), then the full balanced detector system with Schottky-barrier diodes must be employed and the threshold check made every time. Certainly, if measuring a completely new and unknown source, then a careful and complete calibration and determination of measurement threshold must be done.

We have experienced a degradation of Schottky-barrier diodes which we do not pretend to understand.[4] The peak inverse voltage allowable decreases with operating life and some strange noises appear in the demodulator output. This requires replacement of the diodes before taking more data.

A simple operational check for an adequate measurement threshold is worth knowing about. In the calibration procedure, a precision signal frequency attenuator is needed to take the slope data. We leave this attenuator in the system for the balance of the measurement. Regardless of the kind of detection system, increasing attenuation on the input of the demodulator by 3 dB should make the wave analyzer output indicator go down by the same 3 dB. If there is less than 1 dB of change on the wave analyzer output, the system threshold is inadequate. If there is a 2-dB change, taking threshold data and correcting will give a reliable answer.

One method of reducing AM threshold [4], [5] has been thoroughly evaluated by Fikart *et al.* [9]–[11] and found to be of dubious utility. Essentially, the cavity discriminator [3]–[5] can be used for AM noise measurements by inserting a 90° phase shift in the reference line going to the output phase detector. Component imperfections and drift of the source and/or the discriminator cavity tuning cause sufficient errors to make this a method of last resort. Since only the two-resonator klystron oscillators have approached the threshold of the dual diode system with Schottky-barrier diodes, the method of last resort is not often needed.

When measuring an amplifier or frequency multiplier, AM noise at input and output is measured separately. Since these components usually operate in a highly saturated mode, there is little correlation between input and output AM noise. Furthermore, the AM noise at the output is quite dependent on relative carrier power output. We have observed a tendency to neglect making the AM noise

[4] In a conversation with Dr. John Ondria at the 1976 IEEE-MTT-S International Symposium, he reported similar experiences. The diode manufacturers are aware of the problem and recently produced diodes are better in this regard.

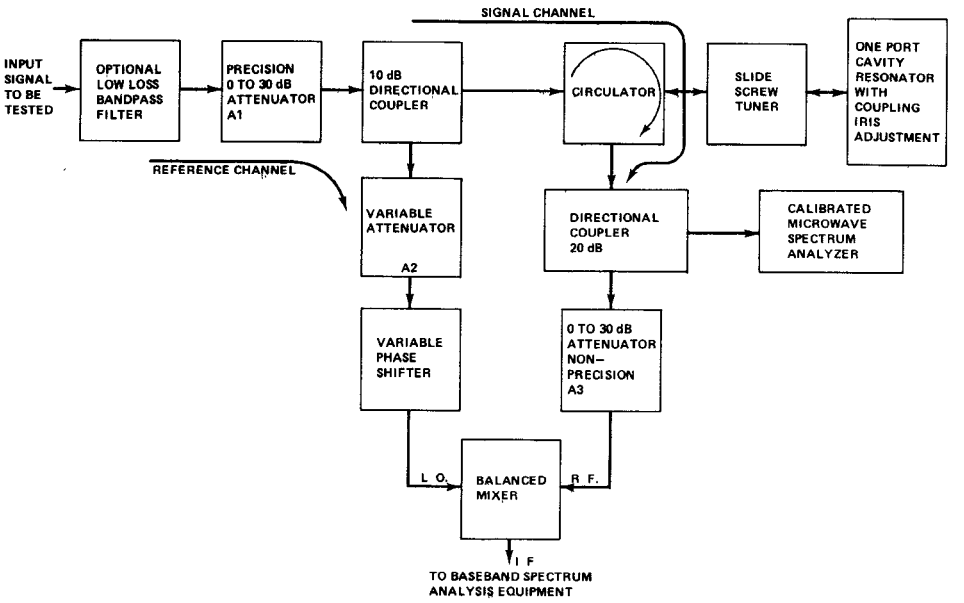

Fig. 9. A microwave frequency discriminator for FM noise measurement.

measurement which is not at all justified by transmitter device performance.

V. Microwave FM Noise Measurements

We will follow the historical development of accepted noise measurement circuits in describing FM or phase noise measurements; thus the discussion in this section will concentrate on the microwave region above about 5 GHz, and the following section will discuss FM noise measurements for carrier frequencies below 5 GHz.

The history is difficult to document because much of the work was classified for security reasons in the era following World War II and during the Korean War. This work has now been declassified, but the archival journal papers were not written at the time, and one would have to delve into company and military reports to adequately give credit to those who made the first contributions. With regard to equipments available in the USA, we can trace a clear path back to the Royal Signals and Radar Establishment (RSRE), Great Malvern, Worcester, England. During the 1950's the RSRE supported the development of klystron oscillators and amplifiers for Doppler radar use. These klystrons quickly presented a measurement challenge, and the apparent result was the development of the cavity discriminator which Whitwell and Williams [12] attribute to "S. B. Marsh, J. D. Clare, and S. A. Drage of RSRE who evolved the frequency discriminator and constructed the first experimental models . . .". This equipment was marketed in the United States by James Scott & Company, Ltd., Glasgow, Scotland, as the Allscott Model 123 Noise Measuring Equipment, and the first author of this paper made his first believable FM noise measurement with Allscott equipment in the early 1960's.

Aside from the fact that it did represent a completely designed equipment with a set of operating instructions, the RSRE discriminator bridge had two superiorities over the prior art: first, it would reject a good amount of incidental AM noise on the test signal; and, second, input power could be increased (with proper adjustment of the equipment) to override the threshold noise in the equipment. Thus the 10-W sort of two-resonator klystron oscillators which still hold the world record for low FM noise could be measured.

Those who use the RSRE cavity discriminator quickly tire of tuning the microwave bridge based on a magic tee or 3-dB four-port directional coupler, and of tuning the klystron used as a local oscillator (LO) for the superheterodyne equipment. Many microwave sources put out 10 mW or more, and the input power sensitivity is not needed. Also, the 3-dB hybrid in the bridge costs a total of 6 dB in threshold or detection slope because the signal goes through the hybrid twice. These factors and the need to measure lower noise sources motivated Ondria [4] first and, working independently, Ashley *et al.* [3] to make significant improvements in this equipment. As shown in Fig. 9, a circulator has replaced the magic tee, and the cavity has been modified to include an adjusting screw on the coupling iris. This simplifies tuning and improves the threshold by nearly 6 dB. Since the intermediate frequency (IF) amplification is not often needed, the LO and IF equipment have been left out in the interest of simplicity. Although the final phase detector could be the magic tee circuit of Fig. 6, we have found it more convenient to use a standard balanced mixer[5] in the discriminator as illustrated in Fig. 10.

There are two approaches to deriving a theory for demodulator circuits such as this frequency discriminator: 1) the quasi-stationary frequency assumption [3]; or, 2) the sideband phasor method [4]. The first has the advantage

[5] Such as a Varian Orthomode® mixer designed as a downconverter for superheterodyne receivers.

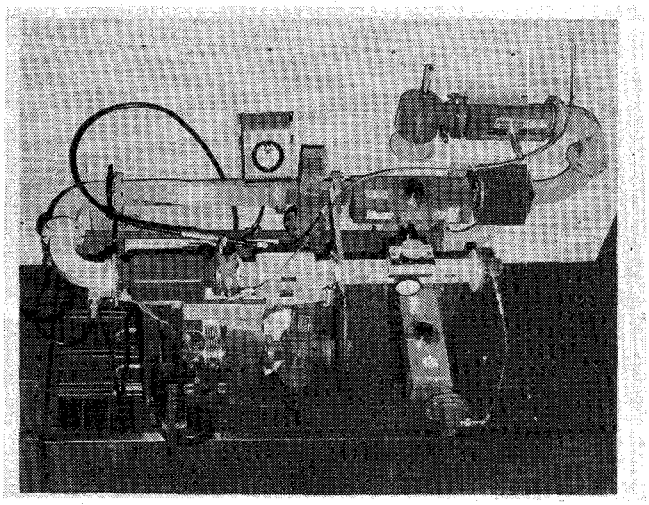

Fig. 10. Photograph of the *C*-band implementation of Fig. 9.

of yielding a direct answer for the discriminator slope and showing that the answer is good for modulation frequency approaching zero; thus we can use the discriminator for short-term and even medium-term stability indications for comparison with other measurement techniques. The second yields the upper modulation frequency correction factors more directly. The first method is the one used in communication theory study of noise problems in FM systems [7].

Either method will yield an equation for the slope S of the form

$$S = \frac{\Delta v}{\Delta \nu} = \frac{K\sqrt{P_i}10^{-(G_H/20)}Q_0}{\nu_c} \tag{39}$$

where

- $\Delta\nu$ small deviation from the carrier frequency (peak hertz);
- Δv small dc change in output (volts);
- P_i input power (watts);
- G_H loss in the system between input and phase detector (decibels);
- Q_0 internal Q of the microwave resonator;
- ν_c carrier frequency (hertz);
- K a factor depending mainly on the conversion loss in the phase detector.

This equation is again one that is mainly for study rather than for actual calculation. The measurement of the factor K has some conceptual difficulties, and we do not need to tell you that measurement of a resonator Q_0 which is probably greater than 20 000 is a challenging problem. Thus most laboratories use a technique based on applying a known angle modulation and measuring Δv to determine S. Such a technique will be described along with the tuning and operating procedure. For now, it is important to draw some conclusions from (39) that influence operation.

First, we note that the slope is proportional to $\sqrt{P_i}$. Therefore, if a calibration is done to determine S, this result is valid only as long as P_i is not changed. All the other factors of (39) are quite stable, and as long as the power is maintained constant, the slope is very stable with time. Therefore, it is quite reasonable to use one source (which might be easy to angle modulate) for calibration to measure another source; all that must be done is to either hold input power constant, or to measure the power ratio and make the appropriate correction.

Second, measurement of a small deviation Δv (corresponding to a quiet oscillator) requires the highest obtainable value of S to override the noise in the crystals of the phase detector. Since carrier frequency ν_c and K are fixed, this means that P_i must be as high as possible, Q_0 high, and G_H minimized. If the circulator shown in Fig. 9 is used, G_H is of the order of 1 dB; whereas the use of a magic tee or 3-dB coupler will make G_H about 7 dB. This 6-dB difference directly translates to a 6-dB lower measurement threshold. If these measures do not result in an adequately low threshold, then methods to be discussed in Section VII must be employed.

In practice, the determination of S is done as part of the tuning and operating procedure, and this will be the organization of our discussion. You will notice that the evolution of signal sources and spectrum analyzers has caused appreciable change in calibration procedure from those reported earlier [3], [4]. In the 1950's and early 1960's, most of the sources being measured were direct microwave oscillators (klystrons, TEO's, IMPATT's, etc.) which could be easily frequency modulated via a bias port. Also, the deviation in these devices could be proved from theory and by measurement to be linear with respect to voltage applied. Microwave spectrum analyzers of that era were not stable and calibration accuracy was low; thus the spectrum analyzer was used to determine the first carrier null and the corresponding modulation index, 2.405. Then the modulating voltage was attenuated by a measured amount and the linearity of the oscillator depended on to calculate the amount of angle modulation used in the calibration. Now, a good fraction of sources to be tested are controlled by VHF or UHF crystal oscillators and usually do not have angle modulation facility. Also, microwave spectrum analyzers have experienced continuous improvement, and now several manufacturers offer equipment with excellent stability and reliable calibration. In particular, the IF attenuator is a stable device that can be accurately calibrated and used as a secondary standard in making the slope calibration. Dynamic range and internal noise in the spectrum analyzer make it possible to measure calibration sidebands 50–60 dB below the carrier with adequate accuracy.

For the discussion of the discriminator tuning, calibration, and operation, we will assume that angle modulation side frequency can be applied to the sources being measured that are 50–60 dB down from the carrier. If the source has internal phase or frequency modulation capability, then the microwave spectrum analyzer is used to measure the side frequency to carrier ratio. If the source cannot be modulated, then a circuit such as the one of Fig. 11 can be connected between source and the discriminator. The idea is simple—amplitude modulation side frequencies with suppressed carrier are generated with a crystal modulator

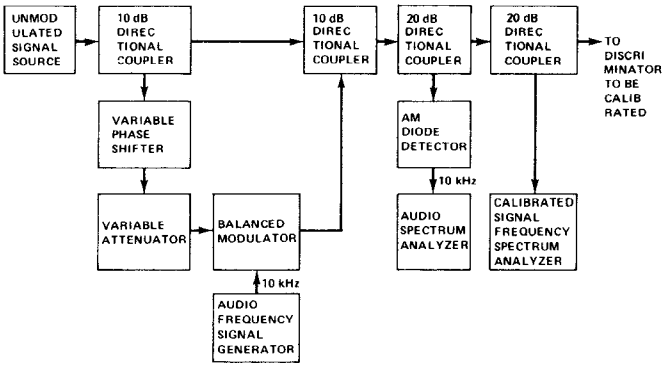

Fig. 11. Generation of angle modulated side frequencies for discriminator calibration.

and reinserted with the needed 90° phase shift to appear as angle modulation side frequencies. The difficulty is to know that the needed 90° phase shift has been obtained and to know if carrier leakage through the balanced modulator will confuse the calibration. The amplitude detector tells us that the phase shifter is set correctly because a simple phasor diagram indicates that minimizing amplitude modulation on the recombined signal is an accurate indication of proper side frequency phasing, even if the balanced modulator has carrier leakage on the order of the side frequencies generated (as has proved the case in modulators we have tested).

During the process of setting up and measuring the calibration side frequencies, the precision input attenuator of Fig. 9 (or Fig. 13) should be set for maximum attenuation to protect the crystals in the balanced mixer.

The operation procedure for the circuit of Fig. 11 is as follows.

1) Apply as much signal frequency power to the input of the balanced modulator as the device will stand without burnout.

2) Set the audio signal generator at the desired side frequency spacing (say, 10 kHz), and adjust the output level while viewing the signal frequency spectrum analyzer. Do not exceed the level which causes second-order side frequencies (at, say, ± 20 kHz) to appear.

3) Tune the audio spectrum analyzer to the frequency of the audio signal generator (say, 10 kHz), and then adjust the variable phase shifter to minimize the indication on the audio spectrum analyzer.

4) Check the level of the angle modulation side frequencies on the calibrated spectrum analyzer.

In operating the circuit, be careful to not burn out the diodes in the balanced modulator with too much RF input or to cause generation of higher order sidebands by the application of excessive audio input power. Usually, it is possible to obtain calibration side frequencies in the range 50–60 dB below the carrier. Side frequencies more than 60 dB below the carrier are getting too close to the internal noise level of the microwave spectrum analyzer to measure accurately enough for calibration purposes. Side frequencies less than 50 dB below the carrier require a modification of Eq. (40).

One clever idea which might occur to you is to use this calibration technique to do a swept calibration of the output indicator; for instance, putting a line of constant side frequency level on the output graph. We have tried this idea with reasonable success. For side frequency spacing greater than 5 kHz, the microwave spectrum analyzer can resolve the sideband structure and prove that the calibration side frequency amplitude does remain constant. On several balanced modulators we have used in Fig. 11, the calibration level line did not behave as expected below 5 kHz, and we were able to isolate the trouble to the balanced modulator. Perhaps a thermal time constant or an unsuspected filter inside the balanced modulator is the cause of the trouble, but our advice is to not to assume the side frequency level is constant if you cannot prove it with the microwave spectrum analyzer.

With the side frequency level set and measured, the discriminator of Fig. 9 is tuned and calibrated as follows.

5) With the reference channel attenuator (A2) set at 0 dB and the threshold check attenuator (A3) set at maximum, decrease the input attenuator (A1) until the reference power at the LO input of the balanced mixer is as high as the mixer will stand without burnout. (A crystal current indicator is a useful way to make this determination.)

6) Replace the cavity resonator with a well-matched termination, and adjust the slide screw tuner for minimum carrier indication on the microwave spectrum analyzer. This cancels undesired leakage in the three-port circulator.

7) Reinstall the cavity resonator and tune to resonance. Check the mode chart and cavity tuning calibration to make certain that the desired mode[6] is being used. The indication of resonance is a dip in carrier level on the microwave spectrum analyzer. Adjust the coupling iris to minimize carrier amplitude, recheck the tuning, etc. Within just a few iterations, the carrier level can be reduced some 60 dB which is more than sufficient. A more important goal to strive for at this stage is to make certain that the resonator is tuned as precisely as possible to the carrier frequency. With the calibration side frequencies present, this is simple to determine because the side frequencies' amplitudes will be the same (the picture is symmetrical) if the resonator is properly tuned. At this stage, it is normal to see the side frequencies' amplitudes within 10 dB of the residual carrier.

8) Reduce attenuator A3 to zero while observing mixer current which should not change. Tune the baseband spectrum analyzer to the modulation frequency of the calibration side frequencies (say, 10 kHz), and adjust the reference channel phase shifter for maximum indication on the baseband spectrum analyzer. (Watch for spectrum analyzer overload.)

9) If the input attenuator A1 is not at 0 dB, increase A2, then decrease A1 until A1 is 0 dB. Recheck the reference phase adjustment. Check for overload in the baseband spectrum analyzer, and insert input attenuation if needed.

[6] These cavities using the TE_{01n} modes are an order of magnitude more difficult to protect from spurious mode troubles than the TE_{111} mode used in cavity wavemeters.

(Here, increasing the precision attenuator A1 by 3 dB should reduce the output indication by 3 dB.)

10) Calculate the discriminator slope S, using

$$S = \frac{\sqrt{2}V_{ac}}{2f_m 10^{-D/20}} \tag{40}$$

where

V_{ac} discriminator ac output voltage at f_m (rms volts);
f_m modulation frequency (hertz);
D side frequency amplitude with respect to carrier frequency amplitude (decibels);

and store this value for later use in data processing.

11) Insert the threshold check attenuator A3, turn off the calibration side frequencies and operate the wave or spectrum analyzer at all frequencies where FM noise data are desired. (The input attenuator of the wave or spectrum analyzer should be set for minimum at this step. An overload light on the input amplifier of the wave analyzer is most useful here.) Record or store these threshold voltages $V_{FTH}(f)$ and the measurement bandwidth B_N.

12) Reduce the threshold check attenuator A3 to 0 dB, check overload of the baseband equipment, and take FM noise data at the desired baseband frequencies $V_{FMM}(f)$. (Use the same values of B_N as in step 11.)

13) Calculate corrected deviation FM(f) at each modulation frequency using:

$$\mathrm{FM}(f) = \sqrt{V_{FMM}^2(f) - V_{FTH}^2(f)}/S. \tag{41}$$

Note that the bandwidth for the measurement B_N was set in the baseband wave analyzer and must be stated along with the values for the FM noise.

14) Convert the FM noise data to other bandwidths, forms, etc.

Several items from our laboratory experience may be helpful to you if you are working on your first or second FM noise measurement. As in the case of AM measurements, we have observed that the most consistent failing is to neglect determining measuring system threshold. We consider the development of threshold checking routines as our most important contribution to the art of noise measurement. If you are attempting to measure a state-of-the-art source with just a few milliwatts output, you will probably find the threshold is too high, and our suggestions for this problem can be found in Sec. VII.

The usual problem is finding a cavity suitable for this use. Cavities intended for use as wavemeters do not have a sufficiently large coupling iris to achieve the critical coupling needed here. Modification is usually not a trivial task. To achieve the high Q_0 needed, the cavity mode is normally from the TE_{01n} family. The TE_{011} will have a $Q_0 \approx 22\,000$ at 10 GHz with a 10-percent tuning range which is moderately free of spurious modes. As the higher order modes are used to obtain higher Q, the spurious mode problem becomes more serious. The vendors most familiar with this kind of cavity resonator are those who develop transmission cavities for oscillator stabilization [14].

Most of the mysteries are found in the baseband equipment. All the good wave and spectrum analyzers have both input and IF attenuators to allow optimization of the level at the first upconverter. These attenuators must be set correctly (as noted in steps 8), 9), 11), and 12)). Some older wave analyzers which were not intended for noise spectrum analysis do not have enough gain in the input stages and a preamplifier is needed.

Another baseband problem is ground loops. When the baseband spectrum analyzer indicates at 60 Hz and harmonics thereof, the question is whether the indication means trouble in the signal source or the measurement apparatus. The threshold check does partially indicate if the indication is in the measurement apparatus because FM from the source will be attenuated by the amount of the threshold check attenuation inserted. Eliminating ground loops seems to be more a matter of experience than anything that is capable of being written down. One source of trouble is the safety ground in the power cords of electronic instruments. All the baseband equipment should be plugged into one box of outlets, and the cords run as a bundle as far as possible. The RF input to the final amplitude or phase detector is best supplied through dc blocks to break up the worst ground loop. Keep in mind that it is the magnetic field that couples into a loop; thus minimizing loop area and placing low-frequency breaks in the loops will minimize current flow.

Minimizing external interference with the measurements is sometimes accomplished by using a shielded room. Our experience has been that this is not as effective as one might think. In general, we have been able to take data in R&D laboratory environments and not find a significant difference if the whole apparatus is moved inside a shielded room. In fact, we have sometimes seen a degradation because the shielded rooms often have ventilation blowers with appreciable acoustic noise output. This acoustic noise vibrates waveguide walls and cavity resonators (as well as the signal source) to cause a messy spectrum below 2 kHz. The threshold check does not distinguish whether this is in the signal source or in the measurement apparatus. If you see a messy spectrum in the FM noise below 2 kHz, turn off all possible blowers and acoustic noise generators to estimate how much of the mess is acoustic. Unfortunately, shielded rooms get hot in just a few minutes after the blower is turned off, and this acoustic noise must be tolerated. One instance where outside interference could not be eliminated without a shielded room was in trying a measurement out on the production floor near a test station for high-power pulsed klystrons. The magnetic radiation from the pulse transformers clearly cluttered the noise measurement on a CW klystron at a nearby test station.

There does seem to be a learning curve associated with making transmitter noise measurements. About a man-week is required to really understand the specification and concept of transmitter noise. After equipment is assembled, another man-week is required to learn the ritual of all the tuning, calibrating, and data taking that must be done. At the end of this second week, you can expect to have some faith in eventually having adequate confidence in the

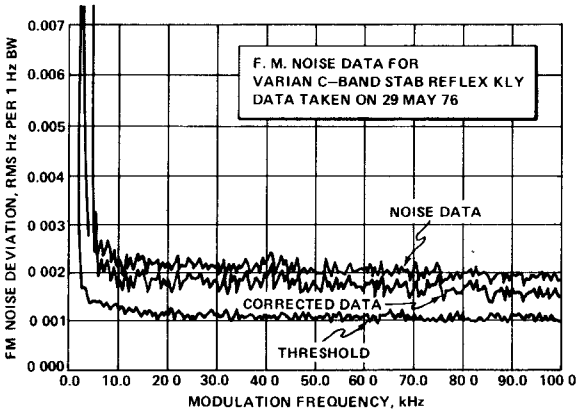

Fig. 12. Typical *C*-band klystron data plot using the HP-3045A automated spectrum analysis system.

measurements. At the end of three to four man-weeks, you can expect enough confidence to tell your superior that the answers are right, and you have mastered the art of transmitter noise measurements. Results such as the typical measurement of Fig. 12 are a pleasure to report.

The use of a frequency discriminator for the measurement of amplifier phase noise might seem inappropriate at first glance. A phase bridge has been used to compare output and input of amplifiers to determine the noise added by the amplifiers. There are several problems with this latter idea. First, an adequately low-noise drive source must be used and the simple phase bridge will not determine adequacy. Second, the threshold will be inadequate if carrier injection is not added. Third, after the measurement results are available, the amplifier noise and driving signal noise have to be combined to find output noise [24].

The frequency discriminator solves all of these problems. Since it is needed for the study of drive source noise, the discriminator is available for studying an appropriate sample of the amplifier output.

The measurement of both AM and FM noise at the output of a 10-W or higher power TWT or klystron will normally show power supply ripple and grounding problems (as seen in Fig. 25). We have reported [25] that the output noise cannot be predicted on the basis of noise figure measurements made at low level and using an IF amplifier at 30 MHz. In the range from 3 dB below to saturated power output, the output noise significantly increases, probably because of RF defocusing of the electron beam and interception on the RF structure.

The complete noise study of a microwave transmitter requires measurement of both AM noise and FM noise at all significant intermediate and output ports. The cavity resonator discriminator just discussed will make the FM noise measurement at the output ports but is not practical for some of the intermediate stages. The next section describes a newly developed technique that is practical for the submicrowave portions of a transmitter.

VI. Submicrowave FM Noise Measurements

The need to make transmitter noise measurements in the lower microwave frequency range, VHF, and UHF ranges has grown because of the evolution of frequency synthesis techniques for microwave transmitters. When a microwave transmitter noise measurement of a synthesized signal yields an unacceptable noise, then one must go back and measure the components used in the synthesis. This was shown to be the case with the Radio Frequency Simulation System developed and installed at the McMorrow Laboratories of the U.S. Army Missile Command, Redstone Arsenal, AL. We found it necessary to make many of our noise measurements below 2 GHz.

The method recommended by Shoaf *et al.* [15] for this frequency range is to electronically phase lock the oscillator under test to a second supposedly identical unit. Then a spectral analysis of the correction voltage in the phase lock loop is the basis for determining the phase noise. To achieve a minimal proof that the oscillators are identical (and that the measured noise can be attributed to each oscillator on a 50–50 basis), a third oscillator is needed so that the three oscillators can be compared two at a time. The need to develop the equipment for the electronic phase locking is a strong disadvantage of this method.

What is needed is a method similar to the cavity discriminator methods described in the previous section. As frequency gets lower, the TE_{011} cavities get larger, and somewhere below 2 GHz attain unreasonable size and weight. (We have not been able to purchase cavities for the region below 5 GHz.) Such a new method must share the following advantages with the RSRE cavity discriminator if the method is to attain bench-mark status.

1) It must be relatively easy to adjust and calibrate.
2) It must be adequately stable in frequency and time.
3) An operational method for determining the measurement threshold must be included.
4) If additional signal power is available, the threshold must be reducible.
5) When properly tuned, the discriminator must reject incidental AM noise on the signal under test.

This need for a new method led us to study transmission line discriminators. These have been known for a long time, but the conventional wisdom for dismissing them was well expressed by Campbell [16] in 1964. "The simplest detector—with the exception of the slope detector—is the interferometer, where the dispersive element is a long line. This is usually used for wide-band applications, with its accompanying low sensitivity. More sensitive versions require an excessively long line and are characterized by multiple responses." The more important faults of prior art transmission line discriminators were that additional input signal power could not be used to reduce threshold and that AM on the test signal was not rejected.

After all the years of operating the microwave discriminator of Fig. 9, it suddenly became obvious that replacing the cavity with a long, shorted transmission line and slide screw tuner, as shown in Fig. 13, gives a discriminator which meets all of the aforementioned requirements.[7] In the VHF range, circulators and slide screw tuners may be hard to obtain while 3-dB four-port hybrid junctions are readily

[7] Three patents [27]–[29] have been issued.

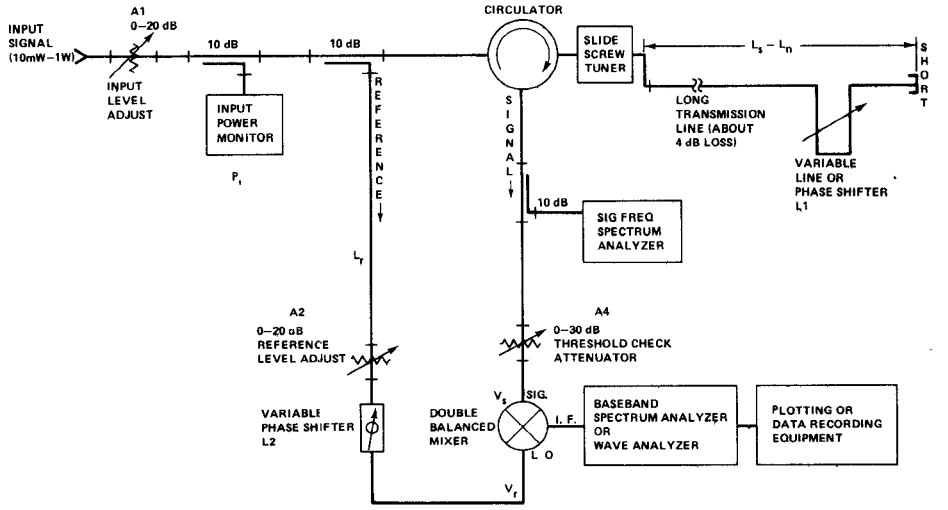

Fig. 13. An optimum sensitivity transmission line discriminator.

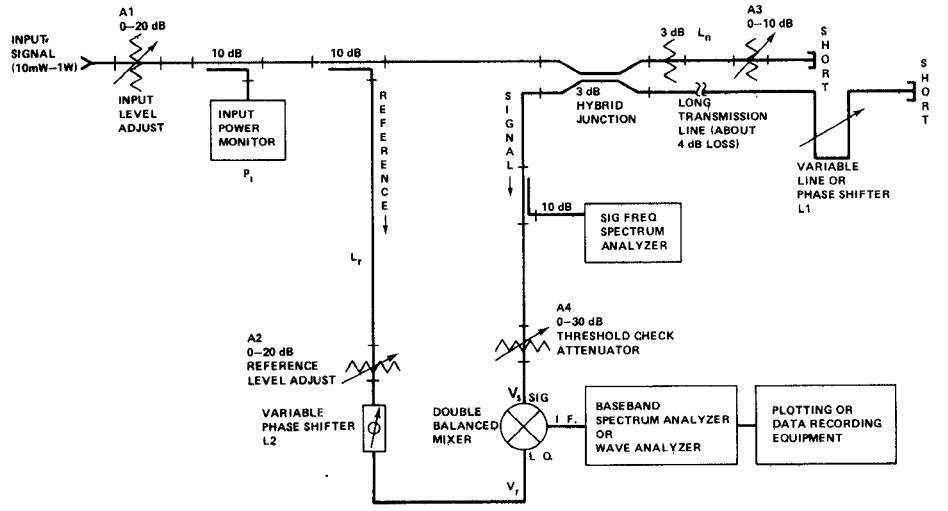

Fig. 14. A wide operating frequency range transmission line discriminator.

available; thus the adaptation shown in Fig. 14 is useful although the threshold and slope are 6 dB poorer than the circulator version.

Although we cannot claim to have looked much further than the ends of our noses, we did not find a published theory to adequately illuminate the use of the transmission line discriminator. Thus we developed some theory of our own which quickly disclosed that all transmission line discriminators have an optimum length for the transmission line. At this optimum length, the signal attenuation is 1 Np.

We have used the quasi-stationary frequency approach to analyze these discriminators. Two transmission line lengths, L_s and L_n, are defined as the mechanical lengths of the signal line and nulling line in either of the discriminators. L_s is the mechanical length of long transmission line and phase shifter in the signal path (m), and L_n is the mechanical length of transmission line in the null circuit path (m). For the discriminator using a circulator and slide screw tuner (Fig. 13) L_n is the distance to the tuner probe. The derivation [22] determines the magnitude and phase angle of the signal applied to the SIG port of the balanced mixer used as a phase detector. Both magnitude and phase angle depends on the depth of the tuning null at v_c as illustrated by Figs. 15 and 16. Using this signal input to the phase detector, we obtain the slope equation

$$S = \frac{\Delta v}{\Delta v} = 8\pi\sqrt{2Z_0P_i}[10^{-(G_M+G_H)/20}](L_s - L_n)e^{-2\alpha L_s}/U_0 \tag{42}$$

where

- Z_0 characteristic impedance of transmission line components (ohms);
- P_i input power to discriminator (watts);
- G_M conversion loss of the balanced mixer (decibels);
- G_H loss in the hybrid junctions between input and SIG port of the phase detector (decibels);
- α transmission line attenuation factor (nepers per meter);
- U_0 phase velocity in the transmission line (meters per second).

This expression for slope does not contain any factors which depend on the depth of the tuning null, which is

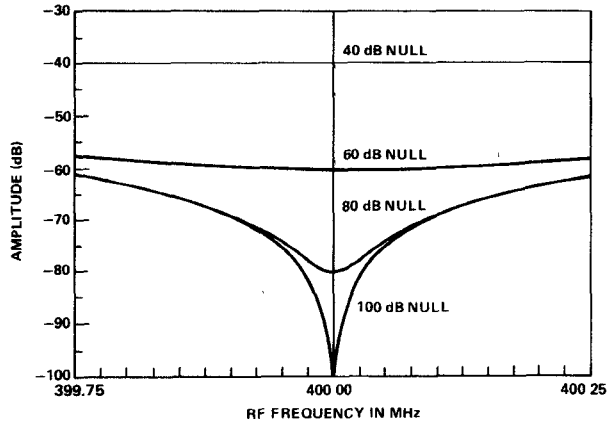

Fig. 15. Amplitude of the signal applied to the SIG input of the phase detector of Fig. 14.

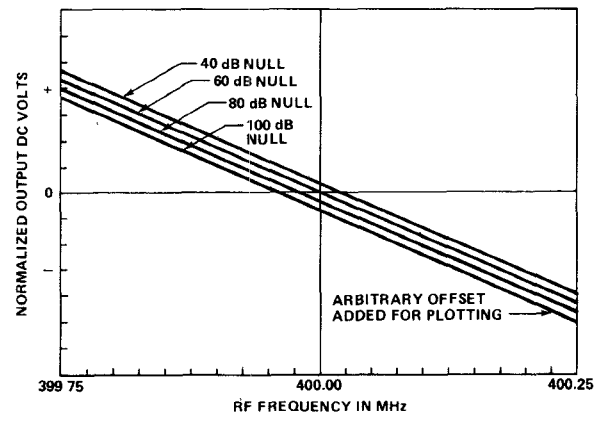

Fig. 17. Output voltage versus input RF frequency for the discriminator of Fig. 14.

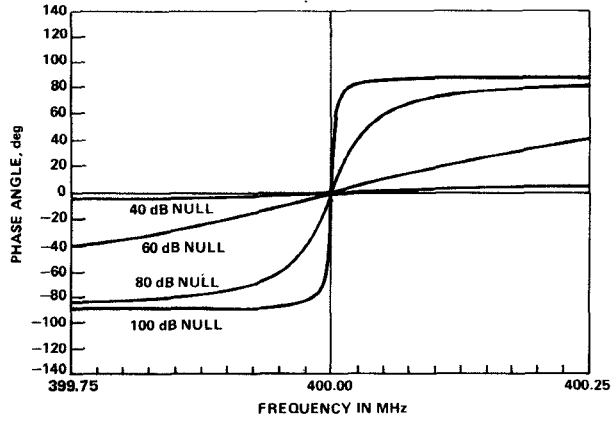

Fig. 16. Phase of the signal applied to the SIG input of the phase detector of Fig. 14.

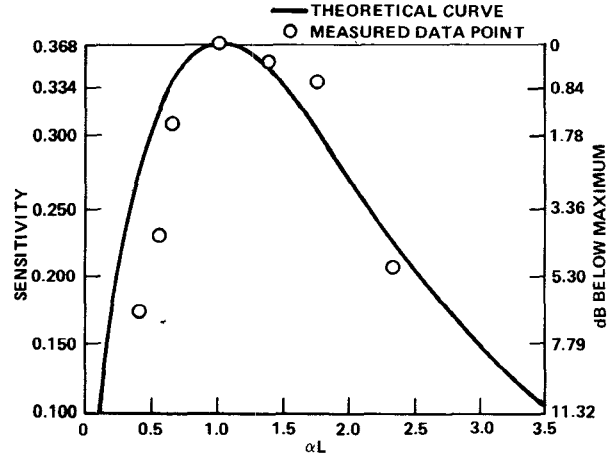

Fig. 18. Sensitivity versus total transmission line length.

surprising in the light of Figs. 15 and 16. Thus we took the expressions which are plotted in Figs. 15 and 16, applied the equation for the phase detector response, and computed the output voltage versus quasi-stationary input frequency in the neighborhood of v_c. Plotting this response yielded curves which fell one on top of the other. An artificial offset was added to make the plots shown in Fig. 17, which clearly shows that the slope does not depend on the depth of the null. This conclusion has been borne out by detailed laboratory measurements.

Any transmission line discriminator has multiple responses. If there are n wavelengths in the long transmission line for the desired tuning, additional nearly equal responses occur for $n + m$ wavelengths where m is an integer. The first adjacent responses are found at

$$v_A = v_c \pm U_0/(2L_s). \tag{43}$$

If this expression is evaluated for the use of an optimum length of low-loss coaxial cable, the adjacent modes are spaced 1 MHz for operation at 100 MHz and spaced 3 MHz for operation at 1 GHz. This spacing is sufficient that FM noise data can be taken through the baseband of interest for Doppler radar (below 100 kHz) without applying correction factors. When measuring TWT's BWO's and other devices without an output filter circuit, a bandpass filter must be used between these sources and any kind of a discriminator.

Notice the analogy between the equations for the slope of the cavity resonator discriminator [see (39)] and the slope of the transmission line discriminator [see (42)]. Both are portiortional to $\sqrt{P_i}$ and energy stored in the system. Both show that amplitude modulation on the input signal is rejected in the output. Perhaps the only surprise is that (42) does not have the factor v_c. Therefore, the transmission line discriminator can be calibrated at one carrier frequency and then used over a ± 5-percent carrier frequency band (with retuning at each value of v_c within the band) without recalibration if P_i is held constant or corrected for.

The slope equation can be normalized and plotted as shown in Fig. 18. Notice that this curve has a maximum at $\alpha L_s = 0.5$ corresponding to a round-trip attenuation of 1 Np (8.68 dB) in the transmission line. Thus we know there is an optimum length for the transmission line which depends only on α, the loss per unit length. The lower the line loss, the longer can be the line and the higher the slope. Our intuition that lower loss line should be better is indeed the truth!

This maximum shown in Fig. 18 is broad enough that a transmission line cut to be optimum at one frequency can

be used over a surprisingly wide carrier frequency range. For coaxial cable below 5 GHz, α is solely dependent on skin depth and changes as $\sqrt{\nu_c}$. Thus for a 3-dB limit on sensitivity (and threshold) degradation, a line optimum at ν_1 can be used from two octaves below ν_1 to three octaves above ν_1.

To verify the aforementioned theory, we have made detailed measurements in the MICOM Laboratories at Redstone Arsenal to confirm Figs. 15–17. Even more gratifying has been the experience in using these transmission line discriminators to make FM noise measurements on sources from 10 MHz to 5 GHz. At 5 GHz, the slope is about 5 dB less than a cavity resonator discriminator with $Q_0 \approx 33\,000$ corresponding to a TE_{013} mode.

The theory and our operating procedure with this transmission line discriminator can be summarized as an alignment, calibration, and operating procedure. Obtaining calibration side frequencies is essentially the same as discussed in steps 1)–4) of Section V, and the discussion need not be repeated here except to indicate it is a required operation. The typical transmission line discriminator shown in Fig. 13 is normally implemented with coaxial components and can be operated over several octaves of input signal frequency range without changing mixer, directional coupler, and the hybrid junction. The alignment and operating procedure can be described in the following steps.

1) Adjust the input attenuator (A1) for approximately 20 mW going into the discriminator. Then adjust the threshold attenuator (A4) for maximum attenuation.

2) Adjust the reference level attenuator (A2) for the proper power level at the input LO port of the mixer. (Normal LO power requirements for mixers of the coaxial type in these frequency ranges vary from 2 to 10 mW). Power level adjustment for these mixers differs from the waveguide mixer in that most coaxial mixers in the 2-GHz and below frequency range do not have a current monitoring capability. For this reason, it has been found that an easy way to set up the mixer LO port power is to disconnect the coaxial cable at the mixer LO port and connect in a power meter. After attenuator (A2) has been set, then reconnect the coaxial cable to the mixer.

3) Adjust phase shifter (L1) at the end of the long transmission line and attenuator (A3) in the other arm of the hybrid for a carrier null as observed on the signal frequency spectrum analyzer. Normally, it is easy to obtain a null on the order of 75 dB. However, nulls as good as 110 dB have been observed. When adjusting for a carrier null, after about 40 dB of nulling has been attained, if the calibration side frequencies have been placed on the carrier, these side frequencies can be used to advantage in determining which direction to adjust the attenuator (A3) and phase shifter (L1). The calibration side frequencies will tend to exhibit an unbalance in amplitude which can be used to adjust the nulling elements. After a relatively few nulling operations it becomes very easy to watch the side frequency amplitude changes and then be able to tell which element should be adjusted and in which direction (i.e., increase or decrease attenuation and more or less phase shift). A properly tuned null will exhibit a carrier with side frequency amplitude not more than 10 dB below the carrier (70 dB null) and both side frequencies will have the same amplitude. The display will be completely symmetrical on the spectrum analyzer used to monitor the nulling operation.

4) Reduce threshold check attenuator (A4) to zero. Reduce input level attenuator (A1) to zero while readjusting reference level adjust attenuator (A2) (remember to use the power meter) to maintain proper mixer LO port power level. Apply angle modulation (if this was not done in the nulling procedure) with an amplitude of 50–60 dB below the incoming carrier and offset from 10 to 20 kHz from the carrier.

5) Locate the modulation frequency on the baseband spectrum analyzer. Adjust variable phase shifter (L2) for a maximum signal output on the baseband spectrum analyzer. Remove the angle modulation calibration signal. (The system is now aligned, calibrated, and ready to take data.)

6) Calibrate the discriminator slope S using (40) presented in step 10) of Section V and store

$$S = \frac{\sqrt{2}V_{ac}}{2f_m 10^{-D/20}} \tag{40}$$

for later use in data processing.

7) Insert maximum threshold check attenuation (A4) and operate the wave analyzer to record the equipment threshold or noise floor.

8) Reduce threshold check attenuator (A4) to zero, check for baseband overload, and operate the wave analyzer, recording the FM noise as the system is operating.

9) If the FM noise measurement is less than 10 dB above the equipment threshold, calculate the corrected deviation at each modulation frequency, using (41).

$$\mathrm{FM}(f) = \sqrt{V_{\mathrm{FMM}}^2(f) - V_{\mathrm{FTH}}^2(f)}/S. \tag{41}$$

Note that the bandwidth for the measurement was set in the baseband wave analyzer and must be stated along with the values for the FM noise.

10) Convert the FM noise data to other bandwidths, forms, etc., as required for the format of presentation desired.

As in the case of the cavity discriminator, the most vexing problem is inadequate threshold. A typical example would be measuring a crystal oscillator directly at 100 MHz or lower frequency. After finding the lowest loss coaxial line that one can afford, the threshold is still too high and the only remedy is to use some form of amplification. (Or, use the two-oscillator method being equally careful to determine threshold.) We need about 30 dB of amplification with power output in the order of 1 W to overcome the threshold problem. This brings up the question "Will the amplifier noise confuse the measurement?" This is the topic of the next section but we will admit for now that our experience indicates that such an oscillator can be measured with an amplifier and transmission line discriminator.

For the total microwave transmitter, we evade this issue by noting that the amplifier is needed to drive the frequency

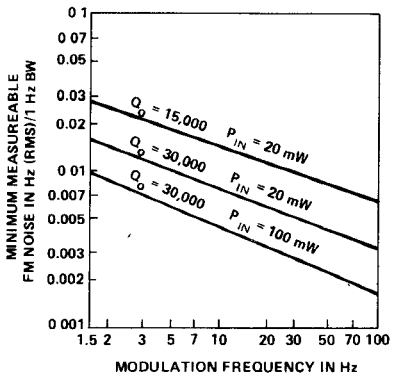

Fig. 19. Threshold level of a 16-GHz FM discriminator. This threshold is set by noise in the phase detector crystals.

multiplier. It is the output of this amplifier which is important, and this can be measured with the discriminator. Once the power is increased and then the deviation increased by the frequency multiplier, we can measure with ease and confidence in the submicrowave and lower microwave regions.

VII. Reduction of FM Noise Measurement Threshold

The problem which has caused the most trouble in the laboratory is the measurement of FM noise on low-power signal sources. At microwave frequencies, noise reduction by transmission cavity stabilization reduces output power by typically 6 dB as well as significantly reducing the FM noise. At submicrowave frequencies, the basic crystal oscillators are operated at relatively low output power, and even after amplification the following frequency multiplier loses power in the process. Yet these sources for microwave signals represent the state-of-the-art in low noise and must be measured.

The discriminator slope equations for both the cavity resonator discriminator [see (39)] and the transmission line discriminator [see (57)] both show that the slope is proportional to $\sqrt{P_i}$ and energy storage (Q of the cavity, length of the line) in the system. The noise generated in the crystals of the phase detector is constant because the LO port input power is held constant. Thus the threshold depends on $\sqrt{P_i}$ and energy storage. For the cavity discriminator, this is illustrated by Fig. 19. After one has used the highest possible cavity Q_0 or the optimum length of lowest loss transmission line, the only way to reduce the measurement threshold is to add amplification to the system. This amplification must be added with care so that the verification of the system threshold is not lost. One useful method for adding this amplification was developed by Ashley and Palka [19].

The usual noise properties of an amplifier (expressed as the noise figure) are not important here because this amplifier must operate at a high carrier level. The important factor is that the amplifier not add FM noise to the signal test. Also, since the discriminator rejects AM, the amplifier can add some AM noise without degrading the measurement. The data published by Ashley and Palka [20] show

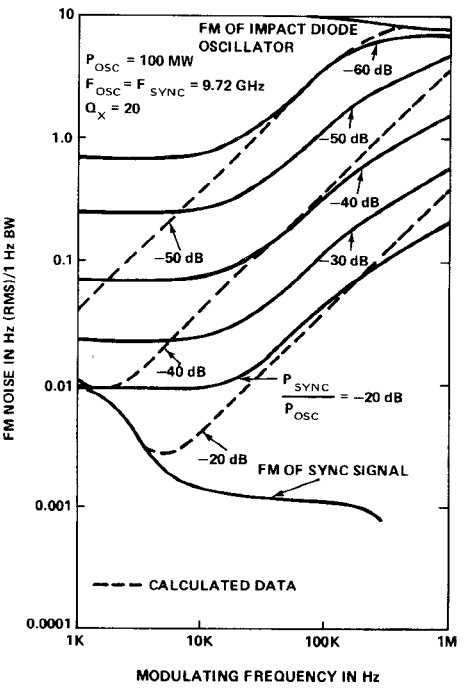

Fig. 20. FM noise in an injection synchronized phase avalanche diode oscillator.

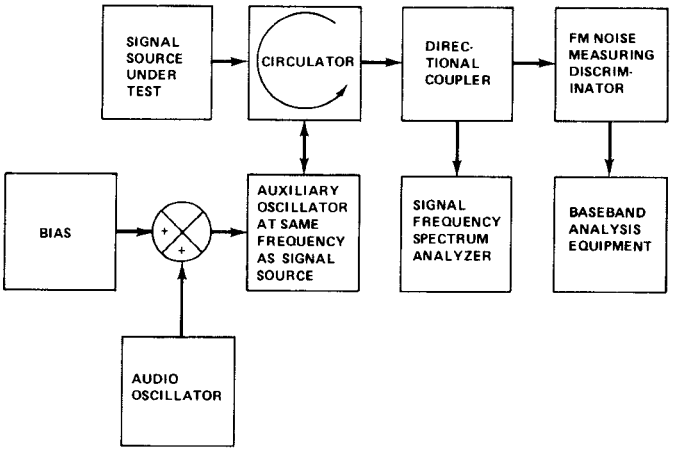

Fig. 21. Use of an injection-locked oscillator to lower the threshold of an FM measurement.

that for a locking gain of about 20 dB, an injection-locked oscillator will reproduce below 100 kHz the FM noise of the locking signal for any but the most sophisticated of signal sources. These data are shown in Fig. 20.

Thus the addition of an injection phase-locked oscillator as an input stage for the FM noise discriminator as shown in Fig. 21 can improve the measurement threshold some 10–20 dB, an improvement which is directly translated to a measurable 10–20-dB lower power signal. As a typical example, consider the use of an auxiliary 100-mW avalanche diode oscillator such as the one in Fig. 20. If we use this oscillator as the input to a discriminator with a cavity Q of 20 000–30 000, comparison of Fig. 19 with Fig. 20 will show that the measurement threshold will be set by the 20-dB curve of Fig. 20. Using an auxiliary oscillator with

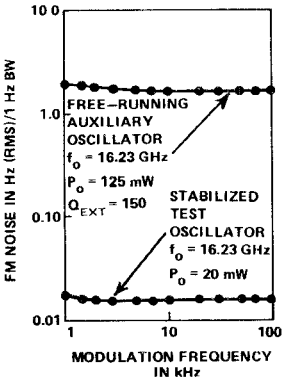

Fig. 22. Typical measurement of a low-noise low-power oscillator.

lower FM noise (higher Q_{ext}) would lower the threshold even more. Most important is the fact that this threshold is achieved with an input power of 1 mW, a level that would be insufficient to operate the discriminator without the auxiliary oscillator. This is a significant improvement.

In addition to improving the measurement threshold, the auxiliary oscillator also makes it much easier to calibrate the discriminator. The usual oscillator can be frequency modulated by applying ac to the bias port. While locked, the result will not be FM but ϕM; but this will be quite satisfactory for calibration purposes because a side frequency level of 50–60 dB below the carrier can be achieved with a symmetrical spectrum indicating pure angle modulation.

A typical result reported by Ashley and Palka [19] is shown in Fig. 22. This oscillator could not have been measured without added amplification of some kind.

We have noted some fear of attempting any kind of an injection phase-locking experiment when we first propose this technique to someone with a threshold problem. This is one of those fears of the unknown which promptly recedes after the experiment is started. Viewing the output of the circulator of Fig. 21 with a signal frequency spectrum analyzer will show the locking process most vividly and quickly will give the needed confidence in the method. We have used the technique often (as has F. M. Palka) and have never experienced any difficulty caused by injection phase locking.

The key idea that made this amplification method work was the availability of theory and measurements for injection phase locking. If another amplification method is to be used as a carrier frequency preamplifier, then it must be understood as well as the injection phase locking. First, we note that this is a high-level output and the usual noise figure measurements and concepts must be used with caution if any degree of output saturation exists. Second, this is a chicken and egg problem because verification of the amplifier contribution requires a known low-noise drive signal. In the case of the injection-lock noise experiment [20], we had available the TE_{015} transmission cavity stabilized two-resonator klystron oscillator to provide the 600 mW needed to make a good measurement of driver source noise.

Going back to the problem postulated at the end of Section VI, the method of attack would be to obtain two 30-dB amplifiers, each capable of about 1-W output power. The crystal oscillator would then drive one amplifier which would in turn drive the second amplifier via a 30-dB attenuator. Comparison of the two amplifier outputs with the transmission line discriminator should tell something about the FM noise added (or hopefully not added) by the second amplifier.

VIII. Baseband Noise Analysis Equipment

The most frequent question asked about transmitter noise measurements is, "Are these measurements repeatable from one laboratory to another?" Our answer to this can be only a qualified "yes" with the qualification being that the personnel making the measurements to be compared have at least several man-months of experience in what is often regarded as a topic with more art than science. When we do run down differences, the usual diagnosis is that the baseband equipment is different. On many occasions in our own laboratories, we have used two different analyzers to study the noise output of a common discriminator and found the answers to be several decibels different on first evaluation. Only careful attention to detail in understanding and calibrating the baseband equipment will resolve these differences.

The signal coming out of either the amplitude or angle demodulator is a function of time; yet the use of time domain analysis equipment is not very common. The use of a storage oscilloscope [3] has proved useful for both medium-term instability display and for the display of pathological misbehavior of signal sources.

Since the usual microwave radar or communications system employs frequency domain processing of the demodulated signals, it is the frequency domain analysis of the residual modulation noise which is most significant to transmitter evaluation and specification. The equipment used has evolved from the wave analyzers of the 1930's developed for the study of audio frequency signals, harmonic distortion in amplifiers, etc. In current terminology, an analyzer which is manually tuned (or perhaps sweep tuned with a motor drive) is called a wave analyzer, while an analyzer which has an electronic sweep of frequency is called a spectrum analyzer. The obvious conflict of terminology is that a sweeping analyzer for displaying the spectrum RF or microwave frequencies is also called a spectrum analyzer. We try to give an idea of the frequency range of the input signal (baseband, RF) whenever using the name spectrum analyzer.

Baseband analyzers operating in the frequency domain can be further classified as either constant bandwidth (say 100 Hz) or constant percentage bandwidth (say 1/3 octave.) Since the theory of noise is rooted in the idea of constant measuring bandwidth and since system noise performance depends on constant incremental bandwidth (i.e., multiplexing a number of 3-kHz channels into a broad baseband signal for transmission), the constant bandwidth analyzers are in far more frequent use although some

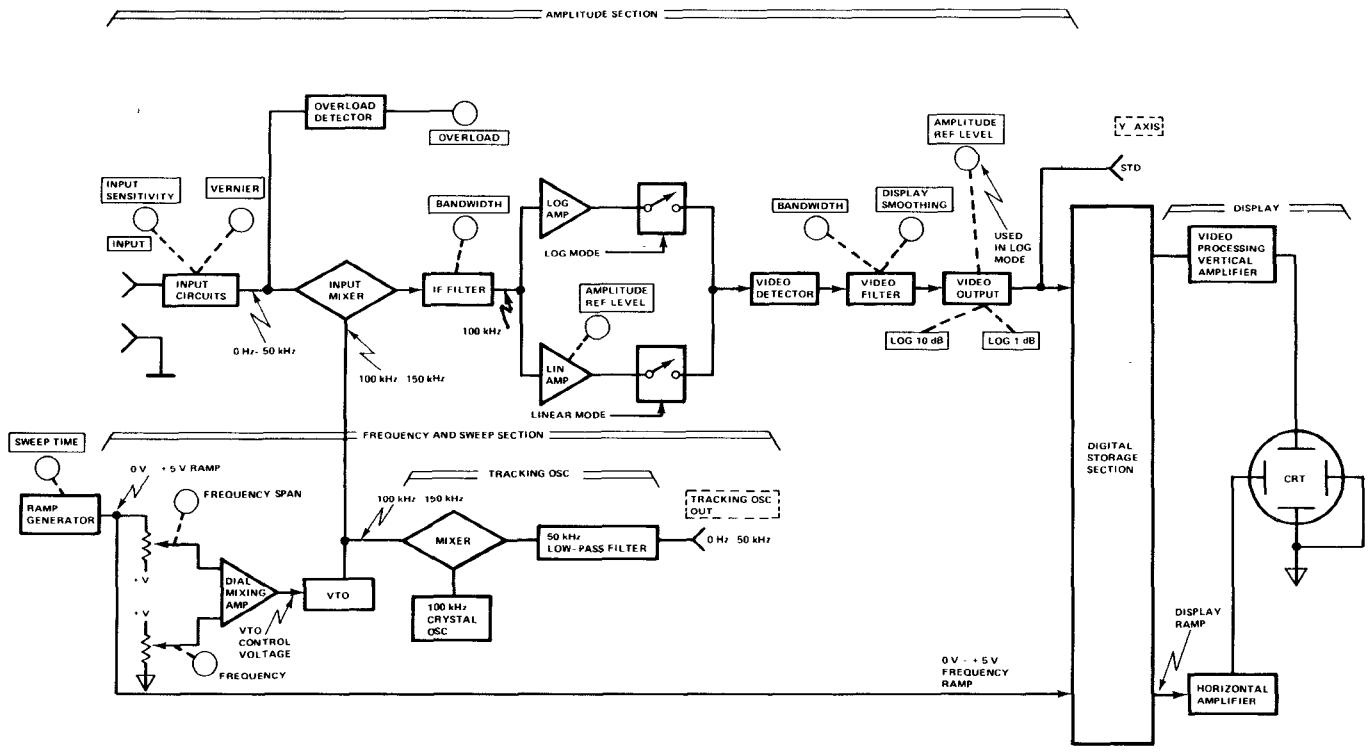

Fig. 23. Simplified block diagram of HP-3580A spectrum analyzer.

operating time convenience could be achieved by correct use of constant percentage bandwidth equipment. In this last category, measurement time can be tremendously reduced by operating parallel banks of overlapping constant bandwidth filters, and this equipment is usually called a real time analyzer.

Digital filtering and processing of noise data to obtain frequency domain information (by use of correlation computation and fast Fourier transform methods) is gaining wide acceptance in environmental studies and audio applications, but has not been used, to our knowledge, for analyzing modulation noise.

The constant bandwidth wave or spectrum analyzers are superheterodyne receivers such as the one shown in the block diagram of Fig. 23. This particular equipment has been selected for discussion because it is typical of all constant bandwidth analyzers and illustrates the basic concepts. Other equipments may use higher IF to accommodate wider input frequency range, but the block diagrams will be remarkably similar.

The input circuits box contains three essential items: 1) the input attenuator system, 2) amplification, and 3) a low-pass filter. The input attenuator is needed when the analyzer is used for relatively high-level input such as during the calibrate or alignment stage of a noise measurement. To minimize the noise contribution of the internal stages of the analyzer, this attenuation must be adjusted to the minimum possible loss for a measurement.

The amplifier is needed to allow measurement of lower level signals such as the noise output from a demodulator. Since the noise figure for an amplifier can be made several decibels better than the noise figure for the mixer, the noise performance of the analyzer can be improved with at least 10 dB of gain in the input amplifier. The amplifier must be used with care because it can be over driven (as can the following mixer) to make a measurement invalid. An input stage overload indicator is a tremendous operational convenience.

The low-pass filter is needed to reject signal components at IF (100 kHz) and in the image band (200–250 kHz).

The mixer converts the input spectrum (0–50 kHz) to sidebands above and below the LO frequency (100–150 kHz). The mixer is balanced to minimize the LO component in the output. The objective is to move the input spectrum past the fixed frequency and relatively narrow bandpass of the IF amplifier and filter. The dynamic range of the analyzer is set in the mixer. The mixer normally works so well that we are not appreciative of the design skill required.

The stability and operational features designed into the LO system, a swept voltage tuned oscillator in our example, are the biggest factors in determining the stability and operational features of the analyzer. We can appreciate these features without detailed study of the circuits.

The IF filter stage sets the measurement bandwidth which is crucial to the accurate analysis of the noise signal. In this analyzer, a five-stage synchronously tuned crystal filter has a bandwidth (between 3-dB points) of 1 Hz. By adding resistive losses and compensating the interstage amplifier gains, the bandwidth can be switched in a 1-3-10 sequence to a maximum of 300 Hz. For this synchronous tuning, the frequency response has the familiar bell shape of the Gaussian function.

The choice of filter shape is usually made on the basis of

measuring a spectrum consisting of a collection of discrete frequencies (rather than noise.) The first decision is the choice of Gaussian or rectangular shape. In sweeping analyzers, the Gaussian shape is preferred for nearly optimum buildup as a sinusoidal signal is swept past the filter. For manually tuned analyzers, the rectangular shape is preferred to allow a minor amount of frequency drift between the source generating the spectrum and the LO in the analyzer.

For noise analysis, the choice is not important. What is important is to know the noise bandwidth of the response shape—a number not normally in the instruction manual. If the frequency response of the amplifier $H(jf)$ is centered at f_0 and is down 40 dB at f_{LO} and f_{HI}, then the noise bandwidth is

$$B_N = \frac{1}{|H(jf_0)|^2} \int_{f_{LO}}^{f_{HI}} |H(jf)|^2 \, df. \tag{44}$$

We have found [21] that about 30 data points defining $H(jf)$ are sufficient for a very simple rectangular rule integration to determine B_N. This must be done for each bandwidth of the analyzer.

Typically, the noise bandwidth is wider than the 3-dB bandwidth. For this analyzer, it is typically 12-percent wider than the measured 3-dB bandwidth.

Another specification of the IF filter shape relates the frequencies at which the filter attenuation is 60 and 3 dB. The ratio of 60-dB bandwidth to 3-dB bandwidth is called the shape factor and is about 10 to 1 for Gaussian-shape filters. This factor determines the spacing between discrete frequencies which can be resolved by the analyzer and the lowest frequency which can be measured without interference from the zero response. As a good rule of thumb, discrete frequencies spaced 15 times the bandwidth can be accurately measured. The minimum frequency which can be measured is of the order of 8 times the IF bandwidth. The cause of this limitation is the leakage of the LO output through the balanced mixer. As the analyzer is tuned to low input frequency, the leaked LO signal rides up the skirts of the IF filter response and registers as an output of the filter which must be classed as an error.

The output of the IF filter is amplified by a bandpass amplifier to increase the voltage enough to adequately override dc drift in the detector circuitry. To increase the dynamic range of the analyzer, attenuators are again used to optimize signal levels in the amplifier.

The logarithmic compression of a decibel vertical scale is most useful for first looks at a signal. The most stable and smooth way to accomplish the logarithmic compression is to perform this operation in the IF amplifier. Thus the spectrum analyzer we have been describing (Fig. 23) has a second IF amplifier, the LOG AMP, which has a dynamic compression range of 120 dB. This amplifier causes us no extra thinking for sinusoidal signal measurement but does exercise the brain cells for noise measurement.

If the input to the spectrum analyzer has a Gaussian probability density function, the output of the narrow-band IF filter also has a Gaussian density function. The nonlinearity of the logarithmic compression changes this density function and thereby changes the power relationship. The result of the compression of the peaks is that a true rms detection circuit will read 1.45 dB less than the correct value. If the LOG AMP is used, then noise readings must be corrected by adding 1.45 dB while sinusoidal readings do not require correction.

After IF amplification, the detector stage produces a dc output proportional to the IF output voltage (or the logarithm for the decibel output mode).

In most analyzers, the detector responds to the time average of the IF output voltage. This is taken care of in the calibration by the well-known ratio of average to rms for a sinusoid. But when used as a noise analyzer, this is in error by 1.05 dB which must be added to the output indication to obtain the effective time average (rms) of the noise. A true rms detector would be better for a noise analyzer.

For the measurement of sinusoidal signals, the dc from the detector is a nice stable value while for noise measurement, it bounces around with the bigger bounces on the narrower IF bandwidths. Post detection filtering (the video filter of Fig. 23) reduces the bounce of the output at the expense of measurement time.

The detected output is used to drive some form of output indicator. In the usual wave analyzer, the indicator is a simple dc voltmeter calibrated to read rms volts and possibly decibels with respect to a stated reference. For the spectrum analyzer, the output indicator is often an oscilloscope with some form of memory. For the analyzer of Fig. 23 the memory is digital with two sections; thus two different frequency sweeps of data can be compared.

All of this digression into nonmicrowave instrumentation must be understood to make effective microwave transmitter noise measurements. Before using a baseband spectrum analyzer, spend a few hours reading the instruction book—it will be time well invested.

IX. Equipment Operation

Once you have decided to make a transmitter noise measurement, decided on the methodology, acquired the necessary equipment, and located a working space, a very significant question arises: What is the sequence of operations? Intuition might guide you through the maze but it is doubtful that the path will be close to optimum; furthermore, if you hope to automate the measurement, the sequence of operations must be thought out in advance and probably worked through on a manual basis to understand the development of automatic routines such as those of the next section.

Our experience is outlined in the operations flow chart of Fig. 24. A similar operations sequence can be developed for AM noise measurements. Discussion of this flow chart will be the basis for sharing our laboratory experience with you.

Once you have the equipment assembled and operating, you have probably found all of the defective equipment and had it repaired. Next, take the time to verify the calibration

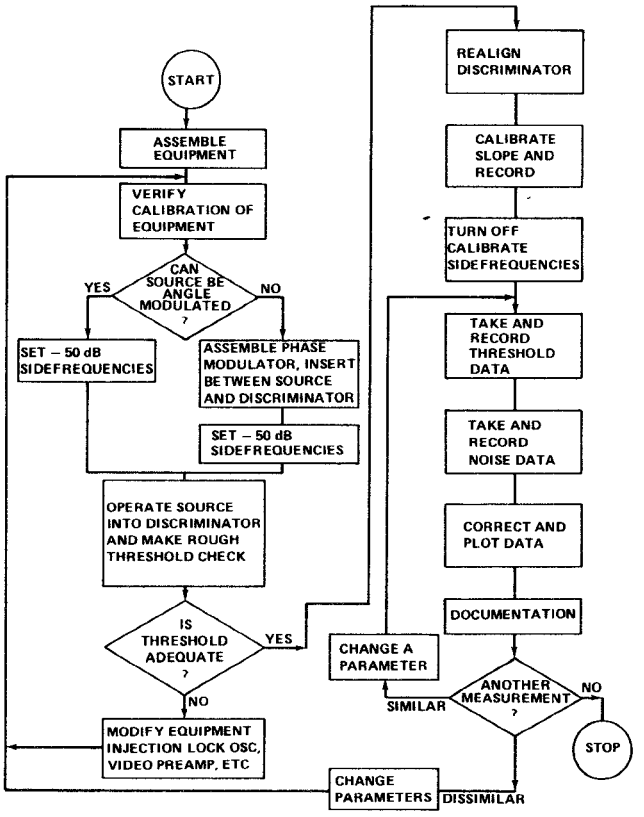

Fig. 24. Operations flow chart for making FM noise measurements.

of the RF spectrum analyzer, power meters, audio oscillators, and precision attenuators. For the RF spectrum analyzer, determine that the IF attenuator calibration is correct. The calibration of the baseband spectrum analyzer will not normally include the noise bandwidth so a separate project needs to be initiated to take the data and do the numeric integration to determine this bandwidth for each position of the bandwidth selector switch. While considering the baseband analyzer, check to see if the IF amplifier is linear or logarithmic and if the detector is average or rms responding. Make note of the necessary correction factors.

Once the source is working and the discriminator has been aligned, a few checks will tell if it is worthwhile to take detailed data. With the calibrate side frequencies on, tune the baseband analyzer to this modulation frequency and check for overload. Operate the input attenuator for maximum sensitivity without overload. If the analyzer does not have an overload indicator, take 10 dB out of the IF attenuator and put in 10 dB with the input attenuator. The output indicator should remain unchanged. If a preamplifier is used ahead of the baseband analyzer, use an oscilloscope to look for clipping at the output. Insertion of 3 dB at the input of the discriminator should make the output indicator fall 3 dB if nothing is overloading.

Turn off the calibration signal and reduce the input attenuator of the baseband analyzer as much as possible without overload. If the output indication is not useful, then remove IF attenuation. If you cannot achieve at least midscale indication at the analyzer output with the minimum bandwidth to be used, then a preamplifier is needed for the input of the baseband analyzer. After this check is passed, drop the input power by 3 dB and note whether the output indicator also drops 3 dB. If it does, the threshold check routine to be done later will yield a negligible correction. If it drops at least 1 dB, there is hope that the threshold check routine will allow correction of the final data to reasonable accuracy. If it drops less than 1 dB, then the threshold is not adequate and either a video preamplifier or the injection-locked oscillator of Section VII must be added.

After you know that the threshold is adequate, then it is worthwhile to take detailed data. If the threshold is more than adequate and you are taking and recording data manually, the slope calibration can be manipulated to make the full scale of the output indicator be a convenient deviation. For instance, the 10-μV full scale might be made equivalent to 10-Hz deviation by clever manipulation of input power and the variable gain knob on the analyzer. At each point where noise data are to be taken, the threshold equivalent deviation or actual voltage, the analyzer bandwidth, and the modulation frequency must be recorded. The same data are taken to determine the noise. Several important factors were written into the step-by-step alignment and operation instructions for the discriminators (steps 8)–13) of Section V and steps 4)–9) of Section VI).

The preceding recording of data is made most convenient if an X–Y recorder can be attached to the wave or spectrum analyzer. This raises the question of how fast the frequency can be swept in taking the data. For noise spectra which are dominated by discrete frequencies (often caused by power supply ripple), the rule is

$$\text{sweep rate} = 0.5\ (\text{bandwidth})^2\ \text{Hz/s} \qquad (45)$$

where the bandwidth is also in hertz. The reason for this rule is that time is required for the high-Q filter in the IF section to build up to the steady state. If the noise spectrum is random and white or pink in shape, then this sweep rate can be multiplied by a factor of 5, which is an appreciable saving in data taking time.

Notice that the sweep rate goes as the square of bandwidth so the largest possible bandwidth should be used. Here is where judgment in taking the data is required. If modulation frequencies below 1000 Hz must be studied, a 10-Hz or smaller bandwidth is needed to resolve power supply ripple components spaced at 50 or 60 Hz and to approach zero frequency as closely as the baseband analyzer will allow. For higher modulation frequency ranges, make a first sweep with a wider bandwidth, say, 100 or 300 Hz. If the result is a white or pink spectrum with no significant humps, the data can be given the final processing and used. If a hump is seen, make a second sweep with the narrowest possible bandwidth and at a sweep rate appropriate for sinusoids. The reason for this advice is shown in Fig. 25. The lump in the curve taken with the 300-Hz bandwidth at 3700 Hz might normally be disregarded as something mysterious in the TWT. Use of the 10-Hz bandwidth and a much slower sweep rate shows that a fine structure related to the 60-Hz power

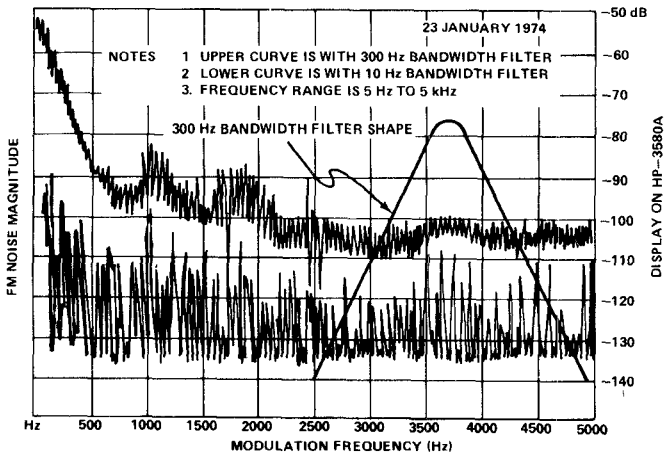

Fig. 25. Modulation frequency (hertz). These data were taken on an HP-3580A using the stabilized klystron as a source to drive a 20-W TWTA.

supply is the cause of this hump. Additional data [22] show that the same spectrum analyzer can detect the ripple components in the TWTA power supply, and a look in the time domain showed switching spikes from the silicon rectifiers were getting past the regulator stage.

Fig. 25 also illustrates several other important facts about spectrum analyzer operation and data interpretation. For the 300-Hz bandwidth data, notice the similarity of the curve below the 500 Hz and the shape of the IF filter response. This is the zero response (helped with a big spectral component at 120 Hz) of the analyzer. In the range above 1500 Hz, a pure random noise spectrum can be measured in one bandwidth and mathematically transformed to another. For these two bandwidths, the curve should be separated by 30 dB which is certainly not true in Fig. 25. Thus, before mathematically transforming bandwidth, take a narrow-band sweep to insure that the spectrum is that of random noise only.

The rules for mathematically transforming noise data to different bandwidths are based on the fact that noise power through a linear filter is proportional to the bandwidth. Thus, if data such as AM noise are taken in decibels with a measurement bandwidth B_N, transformation to another band B_A is accomplished by adding 10 $\log_{10}$ (B_A/B_N). An rms noise deviation is transformed by multiplying by $\sqrt{B_A/B_N}$. We repeat, these transformations are valid only when the noise spectrum is flat over the larger bandwidth.

Measuring an amplifier with a discriminator yields the FM noise $S_{FM}(f)$ at the input and output. To understand the phase noise sources within the amplifier, it is useful to plot the input and output phase modulation noise $S_{\phi M}(f)$. This can be obtained by the use of

$$S_{\phi M}(f) = f^2 S_{FM}(f). \tag{46}$$

The proof of this equation is constructed by remembering the definition of instantaneous frequency [see (3)], and using a well-known theorem of communications theory quoted by Papoulis [8, table 10-1].

One block of Fig. 24 which is often neglected now and lamented later is documentation. Especially when taking data with a sweeping analyzer, record bandwidths, sweep rates, sweep ranges, and something to indicate if the noise measurement threshold is sufficiently low or must be corrected for. Mark the curves for the deviation scale *now*.

The decision block after completing one data run shows a path around the data taking loop which does not include the calibration block. When taking this shortcut path, remember that the calibration remains constant for 5-percent carrier frequency changes and for constant input power.

All the preceding applies to well-behaved portions of a transmitter. While working with klystrons, BWO's, IMPATT oscillators, TEO's, and crystal oscillator controlled sources, we have seen pathological behavior typically in the form of big jumps in the output of the baseband analyzer. The jumps seem to occur at randomly related bands of frequency, but, in truth, are occurring over a wide band of baseband frequencies and coming and going with time. A better indicator is to use a preamplifier and storage oscilloscope to show the time of occurrence of these noise bursts.

X. Automation of FM Noise Measurements

After you have traversed the major and minor loops of Fig. 24 for a few weeks, you will find that you are spending most of your time taking, documenting, and processing data. It is difficult to visualize the complete automation of the noise measurement process but not so difficult to visualize computer control of the noise data taking and processing to significantly reduce operating time.

The first decision is the choice of calculator, minicomputer, microprocessor, or time-shared computer as the controller for the automatic system. For this automation, we have only a few instruments to control and the measurement time is set in the equipment; therefore, blinding speed and large size are not needed in the controller. The calculator has enough size and speed for this job. Our task is similar in size and speed to many other measurement systems, and this class of systems brought about the development of the IEEE Standard #488-1975 Interface Bus for calculator or computer control of measurements and data processing. Using the IEEE Standard #488-1975, the Hewlett-Packard Loveland Instrument Division has developed a spectrum analyzer system for the 10 Hz to 13 MHz range, the HP 3045A system. The controller is the HP 9830A calculator which is programmed in the computing language BASIC. We have been able to write the software to use this system in partially automating transmitter noise measurements.

The organization first divides the tasks into manual or calculator control as shown in Fig. 26. Next, the programming is subdivided on the basis of the operations sequence (Fig. 24). In this sequence, there are branching paths and even the possibility of branching within blocks. Several of the blocks have enough work to be subprograms. One simple way to implement the calculator control is to use the 20 function keys to control the operation of various portions of the program; then much of the branching is accomplished by pressing the appropriate function key.

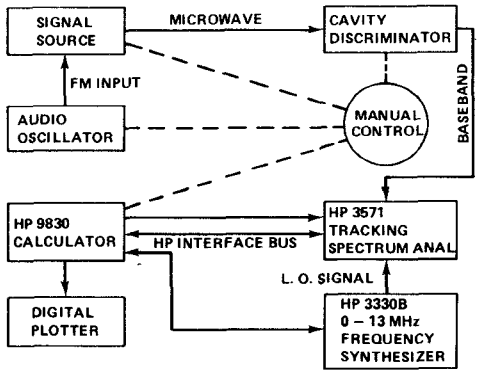

Fig. 26. Automated measurement of near carrier noise.

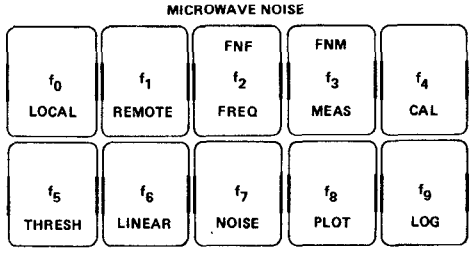

Fig. 27. HP-9830 function keys used to sequence the automated noise measurement.

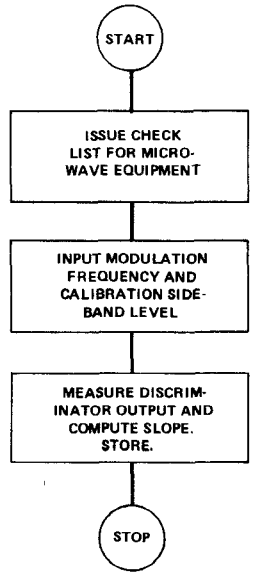

Fig. 28. Flow chart subprogram CAL.

The following subprograms were written and stored on the function keys.

Name	Function
CAL	Calibrates all equipment.
THRESH	Stores threshold data.
NOISE	Takes and stores noise data.
PLOT	Processes and plots noise data.
LINEAR GRID	Draws a linear grid for plotted data.
LOG GRID	Draws a logarithmic grid for plotted data.

The function keys with the appropriate overlay are shown in Fig. 27. Each of these subprograms can be operated independently as far as the calculator is concerned, and this makes possible several noise data runs for one calibrate and threshold run.

Usually, the first step is operation of CAL. The calculator issues control statements and takes data to calibrate the slope (hertz deviation per volt of output) of the microwave discriminator. This is done by applying a small angle modulation to the source under test and adjusting for a known deviation. (The equations to use were given with the discriminator theory.) The result of this calibration is stored in the calculator memory and used in later data processing. The flow chart for subprogram CAL is shown in Fig. 28 and the BASIC program used by the HP 9830A calculator is given in List 1.

```
10  OUTPUT  (13,20)1024;
20  FORMAT B
30  DIM A$[3],B$[36],C$[36],TS[251],NS[251],FS[251],BS[251]
40  DIM D$[10],I$[30],CS[251]
50  DISP "WHAT IS TODAY'S DATE";
60  INPUT D$
70  DISP "WHAT SOURCE ARE U MEASURING";
80  INPUT I$
90  DISP "HAS THE SIGNAL SOURCE WARMED UP";
100  INPUT A$
110  IF A$="NO" THEN 90
120  DISP "IS THE REFERENCE POWER CORRECT";
130  INPUT A$
140  IF A$="Y" THEN 180
150  DISP "SET THE REFERENCE POWER, DIMBULB"
160  WAIT 5000
170  GO TO 120
180  DISP "IS THE REFERENCE PHASE CORRECT";
190  INPUT A$
200  IF A$="Y" THEN 230
210  DISP "TWIDDLE THE PHASE SHIFTER"
220  GO TO 180
230  DISP "HAVE YOU CHECKED INPUT OVERLOAD";
240  INPUT A$
250  IF A$="NO" THEN 90
260  OUTPUT (13,20)768;
270  DISP "WHAT IS CALIBRATE MOD FREQ";
280  INPUT A
290  B=30
300  F=A
310  GOSUB FNF(F) OF 310
320  GOSUB FNB(0) OF 320
330  DISP "HOW MANY DB DOWN ARE SIDEBANDS";
340  INPUT D
350  S=A*2*(10↑(-D/20))/(SQR(2)*Y)
360  B$="THE DISCRIMINATOR SLOPE IS"
370  C$="PK HZ / MICROVOLT"
380  S7=INT(S*1E-04)/100
390  PRINT B$,S7,C$
400  PRINT LIN(3)
410  DISP B$
420  WAIT 2000
430  DISP 97;C$
440  WAIT 5000
450  K1=S/(SQR(2)*1.13)
460  DISP "CALIBRATION IS COMPLETE"
470  END
```

The second step in the measurement sequence is operation of THRESH to determine the noise floor or threshold of the discriminator. The theory is given in Sections V and VI, but the practice is very time consuming because data for the threshold must be taken at each frequency where noise is to be measured. Now the calculator is given the frequency limits for which measurements are desired and the number of data points; then it takes the threshold data and stores the results in an array variable which will be used later to correct actual noise data. Thus all of the measurements can be corrected for threshold before plotting.

The third step is to use NOISE to take data at the same

frequencies where the threshold is known from the previous step. This is completely under the control of the calculator which again stores the results in its memory (as an array variable.) During this step, the human operator can observe the operation of the source under test and the microwave discriminator tuning. Those of us who have spent many hours of tuning a wave analyzer and recording data with pencil and paper especially appreciate the ease of this step.

Probably the most enjoyable step is pushing the calculator key labeled PLOT. This subprogram takes the arrays for threshold and noise, calibration factors, and other corrections to compute threshold corrected noise deviation while the calculator driven plotter plots complete results. Documentation is made painless by answering "yes" to a displayed question, "Do you want to label the axes?" The result is a plot such as the one in Fig. 12 where everything but the caption was put there by the plotter. The linear grid portion was plotted by activating the proper function key. After years of doing noise measurements the hard way, it is pure pleasure to watch the plotter deliver the results of automated noise measurements.

Far more significant than the pleasure of the engineers is the time savings and improved documentation that result from automation. We have proved by personal example that someone familiar with making FM noise measurements manually can learn to operate the automated system in less than an hour. For production line testing, test personnel can be taught to operate this automated equipment much easier than they can be taught to make manual controlled noise measurements and *to do the data processing calculations*. If significant numbers of noise measurements need to be made, then this extra equipment to automate the system will quickly pay for itself.

At the time of this writing, we are at perhaps the 90-percent point on the automation learning curve. It is premature to formally document all of the subprograms and listings; however, we have written this work into a less formal but accessible format [22] which includes all listings ([23] is also helpful).

XI. Concluding Remarks

We listed ten conclusions at the end of the theoretical part of this paper in Section III. We continue with conclusions regarding the experimental technique of making transmitter poise measurements.

1) The measurement of AM noise in all stages of a microwave transmitter is best done with direct diode detectors. The worst pitfall is failing to determine the measurement threshold.

2) The measurement of FM noise for carrier frequencies above 5 GHz is now a repeatable and reliable procedure using the discriminator of Section VI. Be careful in calibrating and determining threshold.

3) The measurement of FM noise for carrier frequencies below 5 GHz can now be accomplished with the improved transmission line discriminator of Section VII. After a few months of operational experience at frequencies between 30 MHz and 5 GHz, we believe the technique is as repeatable and reliable as the methods above 5 GHz.

4) The most difficult FM noise measurement problem is a low-power low-noise source. The use of an injection phase-locked oscillator as a discriminator preamplifier (as described in Section VII) has proved a viable solution for the problem.

5) Most of the problems concerning lack of repeatability from one laboratory to another can be resolved by understanding the baseband analysis equipment.

6) The art of a transmitter noise measurement is in the optimum use of various bandwidths in the wave analyzer.

7) Automation of the measurement is fun (and time consuming) for those doing the work.

8) Not many transmitter noise measurements per month are required to justify the cost of automation.

You will notice two topics we did not discuss. First, the use of two-oscillator techniques for phase modulation noise measurement, and second, pulsed noise measurements. Two-oscillator methods are well described by Shoaf *et al.* [15] and apply more to time and frequency applications than to microwaves. We believe that for submicrowave portions of transmitters, the transmission line discriminator is a more useful tool. With regard to pulsed transmitter noise measurements, we have not yet implemented these and have nothing to add to the work of Sann [24].

Acknowledgment

The work reported in this paper is the result of 26 years of experience by the authors, which makes the task of proper acknowledgment difficult. Whenever we have encountered a theoretical problem, we have either found the answer or a method of attack in the writings of Dr. J. Mullen and Dr. D. Middleton; they deserve commendation for their excellent research. The measurement work which inspired our contributions to this subject has been done in the Gainesville, FL, and Clearwater, FL, laboratories of the Sperry Rand Corporation and the Redstone Arsenal, AL, laboratories of the U.S. Army Missile Command. Without the extensive physical resources of these laboratories, our accomplishments would not be significant. Correspondence and conversations with colleagues too numerous to call by name have added significantly to our knowledge of this topic and equally deserve our heartfelt appreciation.

References

[1] D. Middleton, "Theory of phenomenological models and measurements of fluctuating output of CW magnetrons," *IRE Trans. Elcctron Devices*, vol. ED-1, pp. 56–89, Feb. 1954.
[2] J. A. Mullen, "Background noise in nonlinear oscillators," *Proc. IRE*, vol. 48, pp. 1467–1473, Aug. 1960.
[3] J. R. Ashley, C. B. Searles, and F. M. Palka, "The measurement of oscillator noise at microwave frequencies," *IEEE Trans. Microwave Theory Tech.*, vol. MTT-16, pp. 753–760, Sept. 1968.
[4] J. G. Ondria, "A microwave system for measurements of AM and FM noise spectra," *IEEE Trans. Microwave Theory Tech.*, vol. MTT-16, pp. 767–781, Sept. 1968.
[5] S. B. Marsh and J. D. Clare, "Microwave frequency discriminator," U.S. Patent 3 079 563, Feb. 1963, assigned to James Scott and Company (Electrical Engineers) Limited, Glasgow, Scotland.
[6] J. R. Ashley, T. A. Barley, and G. J. Rast, Jr., "Transmission line discriminators for FM noise measurement," *Proc. IEEE* (Letters), vol. 65, pp. 578–580, Apr. 1977.

[7] D. Middleton, *Introduction to Statistical Communication Theory*. New York: McGraw-Hill, 1960.
[8] A. Papoulis, *Probability, Random Variables and Stochastic Processes*. New York: McGraw-Hill, 1965.
[9] J. L. Fikart, "A theory of oscillator noise and it's application to IMPATT diode oscillators," Ph.D. dissertation, University of Alberta, Edmonton, Canada, Spring 1973.
[10] J. L. Fikart and P. A. Goud, "The direct detection noise measuring system and its threshold," *IEEE Trans. Instrum. Meas.*, vol. IM-21, pp. 219–224, Aug. 1972.
[11] J. L. Fikart, J. Nigrin, and P. A. Goud, "The accuracy of AM and FM noise measurements employing a carrier suppression filter and phase detector," *IEEE Trans. Microwave Theory Tech.*, vol. MTT-20, pp. 702–703, Oct. 1972.
[12] A. L. Whitwell and N. Williams, "A new microwave technique for determining noise spectra at frequencies close to the carrier," *Microwave J.*, vol. 2, pp. 27–32, Nov. 1959.
[13] A. S. Risley, J. H. Shoaf, and J. R. Ashley, "Frequency stabilization of *X*-band sources for use in frequency synthesis into the infrared," *IEEE Trans. Instrum. Meas.*, vol. IM-23, pp. 187–195, Sept. 1974.
[14] J. R. Ashley and C. B. Searles, "Microwave oscillator noise reduction by a transmission stabilizing cavity," *IEEE Trans. Microwave Theory Tech.*, vol. MTT-16, pp. 743–748, Sept. 1968.
[15] J. H. Shoaf, D. Halford, and A. S. Risley, "Frequency stability specification and measurement: High frequency and microwave signals," NBS Tech. Note 632, Jan. 1973.
[16] R. A. Campbell, "Stability measurement techniques in the frequency domain," *Proc. IEEE-NASA Symp. Short Term Frequency Stability*, NASA SP-80, pp. 231, Nov. 1964.
[17] D. B. Leeson, "Short term stable microwave sources," *Microwave J.*, pp. 59–69, June 1970.
[18] J. A. Mullen and D. Middleton, "Limiting forms of FM noise spectra," *Proc. IRE* (Letters), pp. 874–877, June 1957.
[19] J. R. Ashley and F. M. Palka, "Improvement of a microwave discriminator by an injection phase locked oscillator," *IEEE Trans. Microwave Theory Tech.*, vol. MTT-18, pp. 100–101, Nov. 1970.
[20] J. R. Ashley and F. M. Palka, "Measured FM noise reduction by injection phase locking," *Proc. IEEE*, vol. 58, pp. 155–157, Jan. 1970.
[21] T. A. Barley, G. J. Rast, Jr., and J. R. Ashley, "Wave analyzer dynamic range and bandwidth requirements for signal noise analysis," U.S. Army Missile Command Rep. TR-RE-76-26, Mar. 26, 1976.
[22] G. J. Rast, Jr., T. A. Barley, and J. R. Ashley, "Automated measurement of transmitter noise at HF through microwave frequencies," U.S. Army Missile Command Rep. TR-RE-7T-8, in publication.
[23] "Understanding and measuring phase noise in the frequency domain," Appl. Note 207, Hewlett-Packard Instruments Division, Loveland, CO.
[24] K. H. Sann, "The measurement of near carrier noise in microwave amplifiers," *IEEE Trans. Microwave Theory Tech.*, vol. MTT-16, pp. 761–766, Sept. 1968.
[25] J. R. Ashley, T. A. Barley, and G. J. Rast, Jr., "Near carrier noise in TWT amplifiers," *IEEE Int. Electronic Devices Meeting Technical Digest*, p. 599, Washington DC, Dec. 1974.
[26] D. G. McDonald, A. S. Risley, J. D. Cupp, K. M. Evenson, and J. R. Ashley, "Four-hundredth-order harmonic mixing of microwave and infrared laser radiation using a Josephson junction and a mixer," *Appl. Phys. Lett.*, vol 20, p. 296, Apr. 15, 1972.
[27] T. A. Barley, G. J. Rast, Jr., and J. R. Ashley, "Optimum length transmission line discriminator with low noise detector," U.S. Patent 4 002 969, Jan. 11, 1977.
[28] J. R. Ashley, G. J. Rast, Jr., and T. A. Barley, "Optimum threshold transmission line discriminator," U.S. Patent 4 002 970, Jan. 11, 1977.
[29] G. J. Rast, Jr., T. A. Barley, and J. R. Ashley, "Wide operating frequency range transmission line discriminator," U.S. Patent 4 002 971, Jan. 11, 1977.

Design of Stable, Very Low Noise, Cavity-Stabilized IMPATT Oscillators for *C* Band

BERNARD F. VAN DER HEYDEN

***Abstract*—Two types of *C*-band IMPATT oscillators, which easily meet the noise and stability requirements for use as local oscillators in microwave FM communications equipment, are described. Both types use a transmission cavity-stabilization circuit as proposed by Kurokawa. In one of them a TE_{103} mode rectangular invar cavity is used for stabilization, while in the other the coupling is made via a high-*Q* cylindrical TE_{011} mode cavity.**

Although the Si IMPATT diode is inherently noisy, it is shown that a proper choice of circuit parameters and diode characteristics leads to measured FM noise levels of less than 0.2 Hz in a 100-Hz band.

With respect to frequency stability, special attention is paid to hysteresis-free compensation of temperature effects and to the influence of changes with time and ambient temperature of the diode and of the internal atmosphere of the cavity. By careful processing and sealing, an average temperature stability of better than -0.4 ppm/°C was realized with temperature cycling between 26 and 51°C over a period of 450 h.

Manuscript received June 1, 1976; revised September 10, 1976.
The author is with the Product Division Elcoma, Philips Development Laboratories for Transmitting Tubes and Microwave Components, Eindhoven, The Netherlands.

I. Introduction

MICROWAVE signal sources with a high degree of short- and long-term frequency stability find application in systems for radar and FM communication (telephone, television). In many of these systems the local oscillator consists of a crystal-controlled transistor oscillator, followed by a wide-band frequency multiplier, in order to obtain an output signal at the desired microwave frequency. A requirement for the FM noise of the oscillator is set by the CCIR recommendations, which, for example, for an 1800-channel telephone microwave link specify that, measured in a 3.1-kHz band at baseband frequencies from 10 kHz to 10 MHz, the noise level is 80 dB below the level of a 140-kHz rms deviation test tone. If we suppose no preemphasis and no psophometric weighting, this implies a single-sideband FM noise power $\leq$ 10 pW referred to a 1 mW test tone level, or expressed in other units, an rms